A NONLINEAR STABILITY ANALYSIS OF RHOMBIC OPTICAL PATTERN FORMATION IN AN ATOMIC SODIUM VAPOR RING CAVITY

By

FRANCISCO JAVIER ALVARADO

A dissertation submitted in partial fulfillment of
the requirements for the degree of

DOCTOR OF PHILOSOPHY

WASHINGTON STATE UNIVERSITY
Department of Mathematics

AUGUST 2005

To the Faculty of Washington State University:

The members of the Committee appointed to examine the dissertation of FRANCISCO JAVIER ALVARADO find it satisfactory and recommend that it be accepted.

_____

Chair

_____

_____

ACKNOWLEDGMENTS

I would like to thank my adviser, Dr. David J. Wollkind, for his guidance, knowledge and patience, which made this dissertation possible. I would like to thank also the members of my committee, Drs. Valipuram S. Manoranjan and Robert H. Dillon, for their guidance and support.

I thank the faculty and staff of the Department of Mathematics at Washington State for giving me the opportunity to achieve my goals, and my peer graduate students for their friendship and fun moments.

Finally, I thank my wife, Angela Morales, and our children, Bernardo and Josué, for their patience, caring and understanding in these difficult times. Without their encouragement this dissertation would have not been possible.

A NONLINEAR STABILITY ANALYSIS OF RHOMBIC OPTICAL PATTERN FORMATION IN AN ATOMIC SODIUM VAPOR RING CAVITY

Abstract

by Francisco Javier Alvarado, Ph. D.
Washington State University
August 2005

Chair: David J. Wollkind

This dissertation contributes to the theory of optical pattern formation in a purely absorptive medium, namely a resonantly excited two-level atomic sodium vapor system in a ring cavity, by means of a rhombic-planform weakly nonlinear stability analysis applied to the governing time-evolution equation for that phenomenon. In this system, under appropriate conditions, diffraction of radiation can induce the onset of tranverse patterns consisting of stripes and rhombi, in an initially uniform plane-wave configuration. This phenomenon is modeled by a Swift-Hohenberg type-equation describing the intracavity field, and defined on an unbounded spatial domain. This equation is derived from the mean-field ring cavity model of optical bi-stability, generalized to include diffraction. These are complex valued Maxwell-Bloch equations that, under appropriate conditions, can be reduced to a single nonlinear time-evolution partial differential equation for the intracavity field.

Steady-state spatially homogeneous (uniform) solutions of this asymptotic equation are known. The magnitude of the uniform solution and the system's absorption coefficient are the pattern formation parameters. Linear stability analysis shows that only the real part of the solution can be unstable when the absorption coefficient exceeds a critical level. One dimensional analysis shows that supercritical stationary equilibrium patterns occur for an interval of the magnitude of the uniform solution. Two dimensional analysis shows that stripes and rhombi occur depending on the pattern formation parameters. These results are in accord with relevant experimental evidence and numerical simulations.

CONTENTS

LIST OF FIGURES

LIST OF TABLES

Dedication

This dissertation is dedicated to my wife, Angela,

and to our children, Bernardo and Josué.

CHAPTER

ONE

Introduction

Rayleigh-Bénard bouyancy-driven convection has to date provided perhaps the best studied example of nonlinear pattern selection (reviewed by Koschmieder [5]). One of the methods traditionally used to predict such pattern selection is a weakly nonlinear stability analysis that, although incorporating the nonlinearities of the relevant model system, basically pivots a perturbation procedure about the critical point of linear stability theory (reviewed by Wollkind et al. [13]). The advantage of such an approach over strictly numerical procedures is that it allows one to deduce quantitative relationships between system parameters and stable patterns which are valuable for experimental design and difficult to accomplish using simulation alone. Recently, there has been considerable interest generated in pattern formation and selection during the controlled plane-front solidification of a dilute binary alloy under the

influence of an imposed temperature gradient and during chemical reactions occurring in an open gel continuously fed unstirred tank reactor. In order to predict the sequence of interfacial morphologies and Turing patterns actually observed during such solidification and chemical reactions, respectively, Wollkind et al. [14] and Wollkind and Stephenson [15] performed the same weakly nonlinear stability analysis as originally developed by Segel [11] to study Bénard convection cells on the governing systems of a diffusion equations appropriate for modeling these phenomena. In particular all those investigations employed a hexagonal-planform weakly nonlinear stability analysis to determine the relevant parameter range for the transition between one-dimensional and hexagonal pattern formation.

We wish to continue this examination of nonlinear phenomena by investigating spontaneous pattern formation in a ring cavity containing atomic sodium vapor as its optical medium into which a laser pump field is being injected. That passive optical system can be modeled by a Swift-Hohenberg nonlinear partial differential time-evolution equation describing the intracavity field and defined on an unbounded two-dimensional planar domain. The hexagonal-planform weakly nonlinear stability analysis on that model was performed by Edmeade [2]. We will perform a rhombic-planform weakly nonlinear stability analysis and then compare the results obtained with both relevant experimental evidence and numerical simulations as well as place them in the context of some recent pattern formation studies. We begin below with a brief

description of the phenomenon, a sketch of the reduction procedure required to derive the model equation, and a discussion of the methodology to be employed.

1.1 Problem Formulation

This problem is concerned with spontaneous pattern formation in an optical ring cavity containing a purely absorptive two-level atomic sodium vapor medium. Under appropriate conditions, diffraction of radiation can induce transverse patterns consisting of stripes, squares, and hexagonal arrays of bright spots or honeycombs in an initially uniform plane wave configuration [1, 9]. Pattern formation in this phenomenon can be studied theoretically by coupling Maxwell's equation for the intracavity field with the nonlinear Bloch equations for the atomic variables to obtain the nondimensionalized complex system involving the independent variables $t \equiv$ time and $(x, y) \equiv$ traverse Cartesian coordinates with $\nabla^2 \equiv \partial^2/\partial x^2 + \partial^2/\partial y^2$:

$$X_t = -(1 + \mathrm{i}\theta)X + Y - \beta P + \mathrm{i}\chi\nabla^2 X, \tag{1.1a}$$

$$\varepsilon_1 P_t = fX - (1 + \mathrm{i}\Delta)P, \tag{1.1b}$$

$$\varepsilon_2 f_t = 1 - f - (X^* P + X P^*)/2. \tag{1.1c}$$

This set of coupled Maxwell-Bloch equations is the well studied mean-field ring cavity model [3, 7, 10]. Here X and Y are the internal cavity

and injected pump fields; P and f, the atomic polarization and population difference between the upper and lower levels; θ and Δ, the cavity mistuning and atomic detuning parameters; β and χ, the coefficients of absorption and diffraction; and $\varepsilon_{1,2} = \kappa/\kappa_{1,2}$ where κ is the dimensional decay rate associated with X while $\kappa_{1,2}$ bear a similar relationship to P and f, respectively. Further an asterisked quantity denotes its complex conjugate. Steady state spatially homogeneous solutions exist when the pump field, Y, is constant and has no transverse variation. Stable equilibrium patterns arise through instability of these solutions [3]. Should $\varepsilon_{1,2} \ll 1$, as is typically the case, one can employ a steady-state assumption on (1.1b,1.1c) to yield the quasi-equilibrium conditions for the atomic variables (see [3] and Appendix A)

$$f = (1 + \Delta^2)/(1 + \Delta^2 + |X|^2), \tag{1.2a}$$

$$P = (1 - \Delta^2)/(1 + \Delta^2 + |X|^2), \tag{1.2b}$$

where $|X|^2 = XX^*$, which reduces the system of (1.1) to a single nonlinear time-evolution equation that describes the intracavity field X:

$$X_t = -X\left[1 + \mathrm{i}\theta + \frac{\beta(1 - \mathrm{i}\Delta)}{1 + \Delta^2 + |X|^2}\right] + Y + \mathrm{i}\chi\nabla^2 X. \tag{1.3}$$

Equation (1.3) is the two-level generalization of the Kerr cavity, generalized to include diffraction [6]. The limits of validity of this approximation remain a subject of debate; however, for this paper it is assumed that

$\theta = \mathcal{O}(1)$ and the limit $|\Delta| \to 0$ remains regular. Under these conditions the results for θ finite and $\Delta = 0$ are robust enough to approximate well the behavior of a near-resonant ring cavity system [3]. Because the input field is a plane wave, there exists a steady-state spatially homogeneous solution, $X = X_0$, to equation (1.3) when Y is a real positive constant satisfying the steady state equation

$$Y^2 = \alpha[(1 + \beta/\mathcal{D})^2 + (\theta - \beta\Delta/\mathcal{D})^2], \tag{1.4}$$

where $\alpha = |X_0|^2$ and $\mathcal{D} = 1 + \Delta^2 + \alpha$. Equation (1.4) is single valued in Y with respect to α provided $0 < \beta < \beta_{crit}$, where β_{crit} satisfies (see [10] and Appendix B)

$$27\beta_{crit}(1 + \Delta^2)(1 + \theta^2) = (\beta_{crit} - 2 + 2\Delta\theta)^3. \tag{1.5}$$

For the particular values of $\theta = -1$ and $\Delta = 0$, we have that $\beta_{crit} = 10.2$.

Equation (1.4) links the input field intensity Y^2 and the transmitted field intensity α. Graphs of α versus Y^2 are shown in figure 1.1 for several values of β. The shaded region between the vertical lines indicates the interval where optical patterns may form (see section 2.3). For $\beta > \beta_{crit}$ the graph yields an S-shaped curve [7], but in our region of interest, it yields a single valued function.

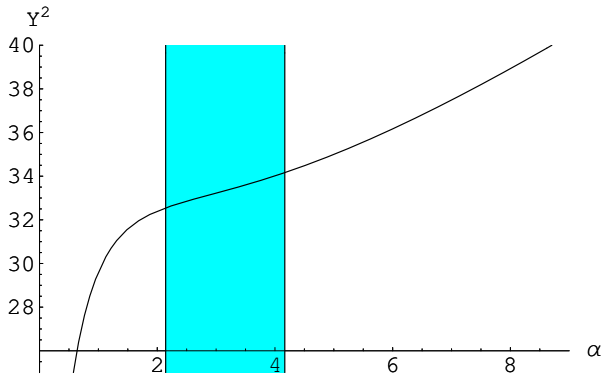

(a) $\beta < \beta_{crit}$

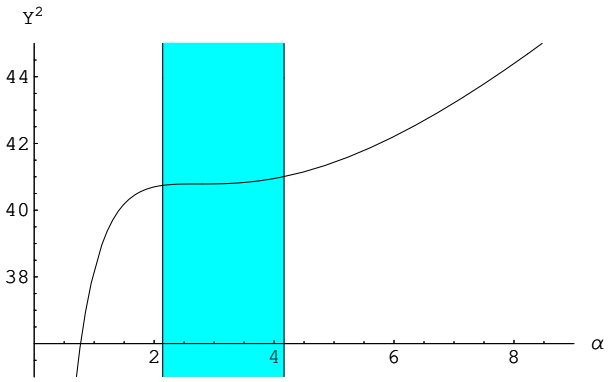

(b) $\beta = \beta_{crit}$

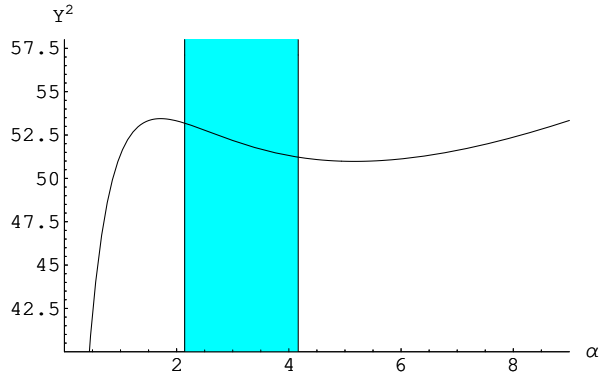

(c) $\beta > \beta_{crit}$

Figure 1.1: Graphs of Y^2 versus α. The shaded region between the vertical lines indicates the interval where optical patterns may form

CHAPTER

TWO

One-Dimensional Analysis

In order to investigate the fate of infinitesimal and finite amplitude disturbances to the uniform state, X_0, we introduce $X = X_0(1 + A)$ into equation (1.3) and retain terms through third order in A to obtain

$$A_t \sim \sum_{n=1}^{3} \sum_{i=0}^{n} \frac{1}{(n-l)!l!} \frac{\partial^n F(0,0)}{\partial A^{n-l} \partial A^{*l}} A^{n-l} A^{*l} + \mathrm{i}\chi \nabla^2 A, \tag{2.1}$$

where

$$F(A, A^*) = -(1 + A)\left[1 + \mathrm{i}\theta + \frac{\beta(1 - \mathrm{i}\Delta)}{1 + \Delta^2 + \alpha(1 + A)(1 + A^*)}\right], \tag{2.2}$$

and

$$A = R + \mathrm{i}I.$$

2.1 Linear Stability Analysis

The linear stability of the uniform solution, X_0, can be investigated when $n = 1$ in equation (2.1) for the one-dimensional situation of $\nabla^2 \equiv \partial^2/\partial x^2$ or

$$\frac{\partial A}{\partial t} = A\left[-1 - \frac{\beta(1+\Delta^2)}{\mathcal{D}^2} + \mathrm{i}\left\{\frac{\beta\Delta(1+\Delta^2)}{\mathcal{D}^2} - \theta\right\}\right] + A^*\left[\frac{\beta\alpha(1-\mathrm{i}\Delta)}{\mathcal{D}^2}\right] + \mathrm{i}\chi\frac{\partial^2 A}{\partial x^2}$$

$$\frac{\partial A^*}{\partial t} = A^*\left[-1 - \frac{\beta(1+\Delta^2)}{\mathcal{D}^2} - \mathrm{i}\left\{\frac{\beta\Delta(1+\Delta^2)}{\mathcal{D}^2} - \theta\right\}\right] + A\left[\frac{\beta\alpha(1+\mathrm{i}\Delta)}{\mathcal{D}^2}\right] - \mathrm{i}\chi\frac{\partial^2 A}{\partial x^2},$$

by employing the following normal mode expansion [6]:

$$[A, A^*] = [k_1, k_2]\,\mathrm{e}^{\sigma t}\cos(qx), \quad \text{where } |k_1|^2 + |k_2|^2 \neq 0, \tag{2.3}$$

which yields the eigenvalue problem

$$\sigma k_1 = \left[-1 - \frac{\beta(1+\Delta^2)}{\mathcal{D}^2} + \mathrm{i}\left\{\frac{\beta\Delta(1+\Delta^2)}{\mathcal{D}^2} - (\theta + \chi q^2)\right\}\right]k_1 + \left[\frac{\beta\alpha(1-\mathrm{i}\Delta)}{\mathcal{D}^2}\right]k_2$$

$$\sigma k_2 = \left[-1 - \frac{\beta(1+\Delta^2)}{\mathcal{D}^2} + \mathrm{i}\left\{\frac{\beta\Delta(1+\Delta^2)}{\mathcal{D}^2} - (\theta + \chi q^2)\right\}\right]k_2 + \left[\frac{\beta\alpha(1+\mathrm{i}\Delta)}{\mathcal{D}^2}\right]k_1,$$

and results in the quadratic secular equation

$$\sigma^2 + 2\left[1 + \frac{\beta(1+\Delta^2)}{\mathcal{D}}\right]\sigma + \delta(\theta + \chi q^2) = 0, \tag{2.4}$$

where

$$\delta(\theta + \chi q^2) = \left[1 + \frac{\beta(1+\Delta^2)}{\mathcal{D}^2}\right]^2 + \left[\frac{\beta\Delta(1+\Delta^2)}{\mathcal{D}^2} - (\theta + \chi q^2)\right]^2 - \frac{\beta^2\alpha^2(1+\Delta 2)}{\mathcal{D}^4}.$$

After Firth and Scroggie [3], we will focus on the resonant-excitation case, $\Delta = 0$, which reduces equation (2.4) to the following equation in σ:

$$\sigma^2 + 2\left[1 + \frac{\beta}{(\alpha+1)^2}\right]\sigma + \frac{(\beta+\alpha+1)[\beta(1-\alpha)+(\alpha+1)^2]}{(\alpha+1)^3} + (\theta + \chi q^2)^2 = 0. \tag{2.5}$$

The marginal curve for equation (2.5) on which $\sigma = 0$ has its lowest threshold in (α, β)-space when $(\theta + \chi q^2) = 0$, that is, when $q = q_c$, with $q_c^2 = -\theta/\chi$. Here q_c^2 is positive and represents the transverse wave number of the most unstable mode. It follows that for $q = q_c$, equation (2.5) has the following roots:

$$\sigma_R(\alpha, \beta) = -1 + \frac{\beta(\alpha-1)}{(\alpha+1)^2} \tag{2.6a}$$

$$\sigma_I(\alpha, \beta) = -1 - \frac{\beta}{\alpha+1}, \tag{2.6b}$$

where σ_R, the growth rate of the most dominant mode, gives the marginal stability curve

$$\beta = \beta_0(\alpha) = \frac{(\alpha+1)^2}{\alpha-1}, \tag{2.7}$$

and σ_I is strongly stabilizing. (See Appendix C for a detailed linear stability analysis on equation (1.1)).

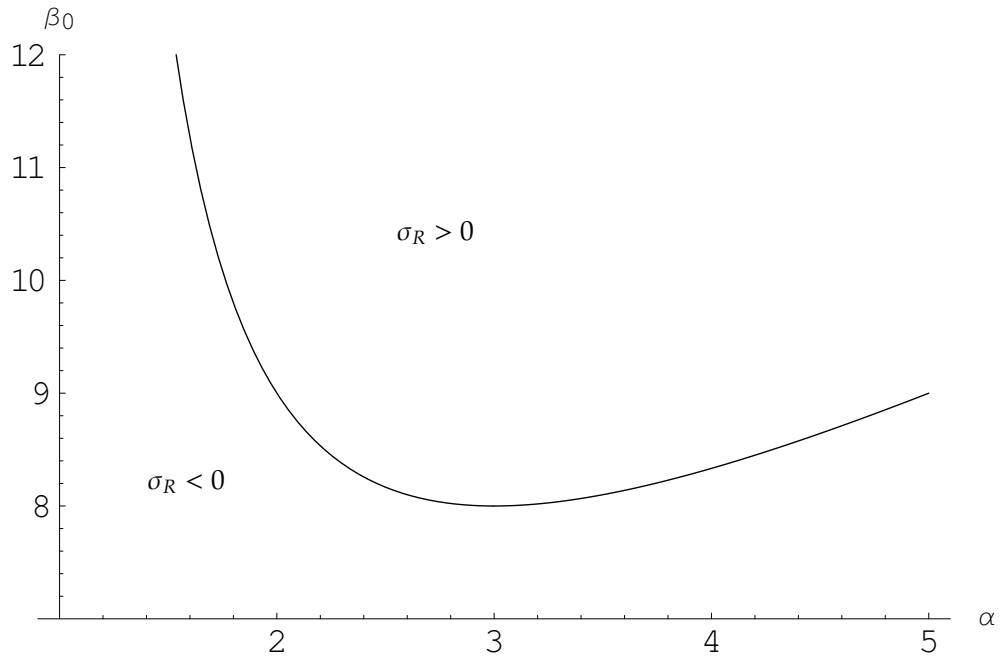

Figure 2.1: Marginal Stability Curve in the α-β Plane

The marginal stability curve shows that the system is unstable for $\beta > \beta_0$ and corresponds to $\left|\theta + \chi q^2\right| \neq 0$. This means that the system becomes unstable when the cavity is mistuned in such a direction that the wavelenght of the light is shorter than that of the nearby cavity mode. These off axis waves can exactly fit the cavity, and it is this fitting requirement that determines the transverse wave vector, q_c, of the most unstable mode [3, 7].

2.2 Swift-Hohenberg Equation

In order to analyze the system's nonlinear behavior we employ the following: substituting $A = R + \mathrm{i}I$ into equations (2.1) and (2.2), and separating real and imaginary parts we derive equations for R_t and I_t which when $\theta = -\chi q_c^2$ have growth rates σ_R and σ_I respectively. Making use of these facts to deduce the quasiequilibrium condition

$$I \sim -\left[\chi/\sigma_I(\alpha,\beta)\right]\left(\nabla^2 + q_c^2\right)R \tag{2.8}$$

from the latter and employing this to eliminate I from the former, we obtain the modified Swift-Hohenberg equation (see Appendix D)

$$R_t \sim \sigma_R(\alpha,\beta)R - \omega_0(\alpha,\beta)R^2 - \omega_1(\alpha,\beta)R^3 + \left[\frac{\chi^2}{\sigma_I(\alpha,\beta)}\right]\left(\nabla^2 + q_c^2\right)^2 R, \tag{2.9}$$

where

$$\sigma_R(\alpha,\beta) = -1 + \frac{\beta(\alpha-1)}{(\alpha+1)^2} \tag{2.10}$$

$$\sigma_I(\alpha,\beta) = -1 - \frac{\beta}{\alpha+1} \tag{2.11}$$

$$\chi q_c^2 = -\theta = 1 \tag{2.12}$$

$$\omega_0(\alpha,\beta) = \frac{\beta\alpha(\alpha-3)}{(\alpha+1)^3} \tag{2.13}$$

$$\omega_1(\alpha,\beta) = \frac{\beta\alpha[8\alpha - (\alpha+1)^2]}{(\alpha+1)^4}. \tag{2.14}$$

According to Firth and Scroggie [3], this equation displays all the essential features of the system, and qualitatively explains all their numerical results. Equation (2.9) is valid only where the spatial spectrum of R is concentrated around $q = q_c$.

2.3 Nonlinear Analysis

In order to investigate the stability of the steady state uniform solution, X_0, to one dimensional perturbations we assume the following nonlinear expansion to the model equation:

$$R \sim A_1(t)\cos(q_c x)+A_1^2(t)[R_{20}+R_{22}\cos(2q_c x)]+A_1^3[R_{31}\cos(q_c x)+R_{33}\cos(3q_c x)]. \tag{2.15}$$

The amplitude function is given by:

$$\dot{A}_1(t) \sim \sigma A_1(t) - a_1 A_1^3(t), \tag{2.16}$$

where q_c is the critical wave number of linear stability theory, σ is the growth of the most dominant mode, and a_1 is the Landau constant [13].

The nontrivial critical point of the amplitude function is given by:

$$A_1^2 = \frac{\sigma}{a_1}.$$

This critical point exists when σ and a_1 have the same sign. The system is subcritically unstable for σ and a_1 negative, and the system re-equilibrates supercritically for σ and a_1 positive. The latter corresponds to pattern formation [13], *i.e.*, finite amplitude perturbations change the system from the linearly unstable uniform state to a stable nonuniform state.

Substitution of the expansions of equations (2.15) and (2.16) into equation (2.9) results in a sequence of problems (see Appendix E), one for

each pair of values of m and n corresponding to a term of the form $A_1^m(t)\cos(nq_c x)$:

- The $m = n = 1$ problem gives the linear theory result

$$\sigma = \sigma_R.$$

- The $m = 2$ and $n = 0$ problem yields

$$R_{20} = \frac{\omega_0/2}{\sigma_I^{-1} - \sigma_R}.$$

- The $m = 2$ and $n = 2$ problem yields

$$R_{22} = \frac{\omega_0/2}{9\sigma_I^{-1} - \sigma_R}.$$

- The $m = 3$ and $n = 1$ problem yields

$$3\sigma R_{31} - a_1 = \sigma_R R_{31} - \omega_0(2R_{20} + R_{22}) - \frac{3\omega_1}{4}.$$

To evaluate the Landau constant a_1 we employ a Fredholm-type solvability condition in the limit as $\beta \to \beta_0$. This yields

$$a_1 = \left[\omega_0(2R_{20} + R_{22}) + \frac{3\omega_1}{4}\right]\Bigg|_{\beta=\beta_0}$$

which implies

$$a_1(\alpha) = \frac{\alpha\beta_0(\alpha)}{(\alpha+1)^4}\left\{-\frac{19}{9}\left[\frac{\alpha(\alpha-3)}{\alpha-1}\right]^2 + \frac{3}{4}\left[8\alpha - (\alpha+1)^2\right]\right\}.$$

From the graph of a_1 versus α shown in figure 2.2 we see that $a_1 > 0$ when $\alpha_1 = 2.14306 < \alpha < 4.16712 = \alpha_2$. Figure 2.1 shows $\sigma_R > 0$ when $\beta > \beta_0$. Since instabilities arise only if $\beta > \beta_0$ we can conclude that the system re-equilibrates supercritically for $\alpha \in (2.14306, 4.16712)$. It follows that stable equilibrium patterns form for this range of α.

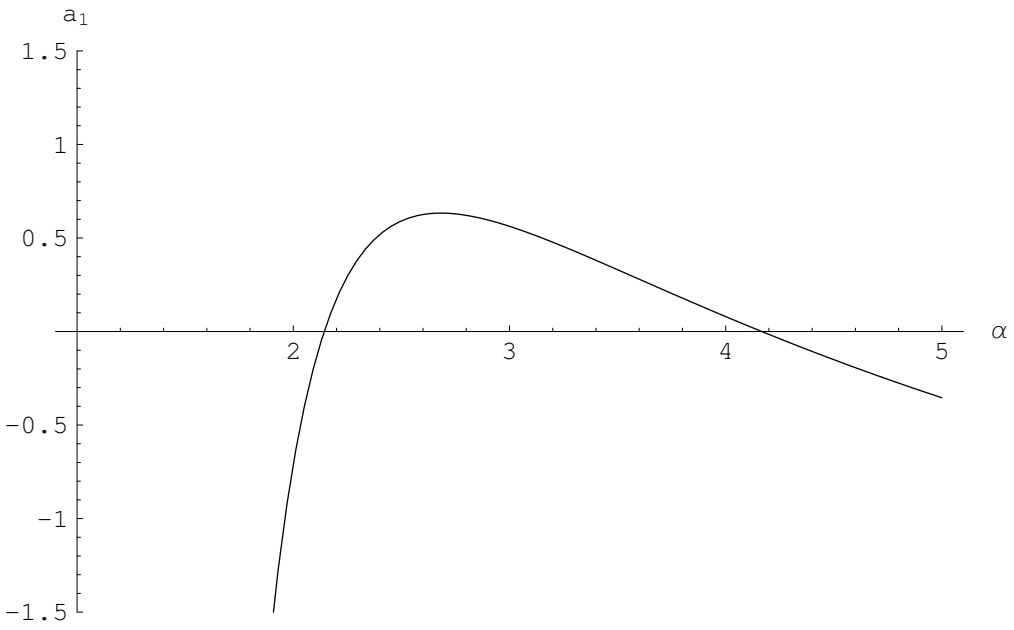

Figure 2.2: Plot of a_1 versus α

CHAPTER

THREE

Two-Dimensional Analysis

One-dimensional analysis reveals that spontaneous pattern formation occurs in the ring cavity system when $\alpha_1 = 2.14306 < \alpha < 4.16712 = \alpha_2$. That is, the system is supercritically stable for the nondimensional square of the uniform steady-state intracavity field in this range, and the nondimensional absorption coefficient such that $\beta > \beta_0$. While one-dimensional analysis reveals the parameter values for which the system is supercritically stable, and corresponds to pattern formation, we are interested in the types of patterns that exists for α in this range.

3.1 Rhombic-Planform Analysis

In order to investigate the possibility of occurrence of rhombic patterns, we seek a solution of our model equation of the form

$$\begin{aligned} R(x,y,t) \sim A_1(t)\cos(q_c x) + B_1(t)\cos(q_c z) + A_1^2(t)R_{20}(x) + A_1(t)B_1(t)R_{11}(x,z) + \\ + B_1^2(t)R_{02}(z) + A_1^3(t)R_{30}(x) + A_1^2(t)B_1(t)R_{21}(x,z) + \\ + A_1(t)B_1^2(t)R_{12}(x,z) + B_1^3(t)R_{03}(z), \end{aligned} \quad (3.1)$$

where

$$\begin{aligned} z &= x\cos(\psi) + y\sin(\psi) \\ R_{20}(x) &= R_{2000} + R_{2020}\cos(2q_c x) \\ R_{11}(x,z) &= R_{1111}\cos[q_c(x+z)] + R_{111(-1)}\cos[q_c(x-z)] \\ R_{02}(x) &= R_{0200} + R_{0202}\cos(2q_c z) \\ R_{30}(x) &= R_{3010}\cos(q_c x) + R_{3030}\cos(3q_c x) \\ R_{21}(x,z) &= R_{2101}\cos(q_c z) + R_{2121}\cos[q_c(2x+z)] + R_{212(-1)}\cos[q_c(2x-z)] \\ R_{12}(x,z) &= R_{1210}\cos(q_c x) + R_{1212}\cos[q_c(x+2z)] + R_{121(-2)}\cos[q_c(x-2z)] \\ R_{03}(x) &= R_{0301}\cos(q_c z) + R_{0303}\cos(3q_c z), \end{aligned}$$

and A_1, B_1 satisfy the amplitude equations

$$\frac{\mathrm{d}A_1}{\mathrm{d}t} \sim \sigma A_1 - A_1(a_1 A_1^2 + b_1 B_1^2) \tag{3.2a}$$

$$\frac{\mathrm{d}B_1}{\mathrm{d}t} \sim \sigma B_1 - B_1(b_1 A_1^2 + a_1 B_1^2). \tag{3.2b}$$

Here we are employing the notation R_{jlmn} for the coefficient of each term of (3.1) of the form $A_1^j B_1^l \cos[q_c(mx + nz)]$.

3.2 Determination of the Landau Constants

In order to determine the Landau constants, we substitute the expansion of equation (3.1) into equation (2.9). Solving the resulting sequence of problems (see Appendix F), we find that

$$\begin{aligned}
\sigma = \sigma_R &= -1 + \frac{\beta(\alpha-1)}{(\alpha+1)^2} \\
R_{2000} &= -\frac{\omega_0/2}{\sigma_R - \sigma_I^{-1}} \\
R_{2020} &= -\frac{\omega_0/2}{\sigma_R - 9\sigma_I^{-1}} \\
R_{1111} &= -\frac{\omega_0}{\sigma_R - \sigma_I^{-1}[1+2\cos(\psi)]^2} \\
R_{111(-1)} &= -\frac{\omega_0}{\sigma_R - \sigma_I^{-1}[1-2\cos(\psi)]^2}
\end{aligned}$$

and that the Landau constants, a_1 and b_1, satisfy the following:

$$3\sigma R_{3010} - a_1 = \sigma_R R_{3010} - (2R_{2000} + R_{2020})\omega_0 - \tfrac{3}{4}\omega_1 \tag{3.3a}$$

$$3\sigma R_{2101} - b_1 = \sigma_R R_{2101} - (2R_{2000} + R_{1111} + R_{111(-1)})\omega_0 - \tfrac{3}{2}\omega_1. \tag{3.3b}$$

Taking the limit as $\beta \to \beta_0$ in equation (3.3) yields the following expressions for the Landau constants:

$$a_1 = \frac{\alpha\beta_0(\alpha)}{(\alpha+1)^4}\left\{-\frac{19}{9}\left[\frac{\alpha(\alpha-3)}{\alpha-1}\right]^2 + \frac{3}{4}\Big[8\alpha - (\alpha+1)^2\Big]\right\} \tag{3.4}$$

$$b_1 = \frac{\alpha\beta_0(\alpha)}{(\alpha+1)^4}\left\{-2\left[\frac{\alpha(\alpha-3)}{\alpha-1}\right]^2\left[\frac{3+16\cos^4(\psi)}{\Big(1-4\cos^2(\psi)\Big)^2}\right] + \frac{3}{2}\Big[8\alpha - (\alpha+1)^2\Big]\right\}. \tag{3.5}$$

We can see from these equations that if $\alpha = \alpha_c = 3$, $b_1 = 2a_1$, and so b_1 does not depend on ψ.

3.3 Amplitude Equations

Having developed this formulae for the Landau constants, we now turn our attention to the rhombic planform amplitude equations (3.2) which possess the following equivalence classes of critical points $A_1(t) = A_0$, $B_1(t) = B_0$:

$$\text{I} : A_0 = B_0 = 0; \tag{3.6a}$$

$$\text{II} : A_0^2 = \sigma/a_1,\ B_0 = 0; \tag{3.6b}$$

$$\text{V} : A_0 = B_0, \text{ with } A_0^2 = \sigma/(a_1 + b_1). \tag{3.6c}$$

Equivalence classes III and IV will be dealt with in chapter 4.

Assuming that $a_1, a_1 + b_1 > 0$ and investigating the stability of these critical points by seeking a solution of (3.2) of the form

$$A_1(t) = A_0 + \varepsilon c_1 e^{pt} + \mathcal{O}\left(\varepsilon^2\right),\ B_1(t) = B_0 + \varepsilon c_2 e^{pt} + \mathcal{O}\left(\varepsilon^2\right),\ \text{with } |\varepsilon| \ll 1, \tag{3.7}$$

one finds that the equation satisfied by p has the associated roots (see Appendix G)

$$\text{I} : p_{1,2} = \sigma, \tag{3.8a}$$

$$\text{II} : p_1 = -2\sigma, \quad p_2 = (1 - b_1/a_1)\sigma, \tag{3.8b}$$

$$\text{V} : p_1 = -2\sigma, \quad p_2 = 2(b_1 - a_1)\sigma/(a_1 + b_1), \tag{3.8c}$$

which yield the stability criteria that I is stable for $\sigma < 0$; II, for $\sigma > 0$, $b_1 > a_1$; and V, for $\sigma > 0$, $a_1 > b_1$.

Note that I and II, as in the one-dimensional analysis, represent the undisturbed and striped states, respectively, while V can be identified with a rhombic pattern (see section 3.6). Note also that these three states are mutually exclusive, that is, no two states are stable in the same region of parameter state.

3.4 Pattern Formation Predictions

In this section we use the stability criteria above to find α-intervals where rhombic patterns arise. Toward this end, we examine the signs of $a_1 + b_1$ and $b_1 - a_1$ for $\alpha_1 < \alpha < \alpha_2$ and $0 < \psi \leq \pi/2$, with $\pi/2$ (or equivalently $90°$) representing a square planform.

We first illustrate this procedure for a few fixed values of α by plotting $a_1 + b_1$ and $b_1 - a_1$ versus α. We also plot a_1 and b_1 for the sake of completeness. In these graphs, the two α-intervals of stable rhombic patterns, where $a_1 + b_1 > 0$ and $b_1 - a_1 < 0$, are denoted by shading, while table 3.1 summarizes our results. Observe that for the α values between these intervals, $a_1, b_1 - a_1 > 0$ and hence there exist stable stripes, while for those to the left of the left-hand interval and to the right of the right-hand one no patterns are predicted by this analysis.

ψ	α-intervals
$\frac{\pi}{6}$	[2.21497, 2.31534], [3.87633, 4.04226]
$\frac{\pi}{4}$	[2.39792, 2.57094], [3.49943, 3.74739]
$\frac{5\pi}{12}$	[2.35493, 2.52338], [3.56465, 3.81365]
$\frac{\pi}{2}$	[2.21497, 2.31534], [3.87633, 4.04226]
$\frac{7\pi}{12}$	[2.35493, 2.52338], [3.56465, 3.81365]

Table 3.1: α-intervals of stable rhombic patterns for different values of ψ

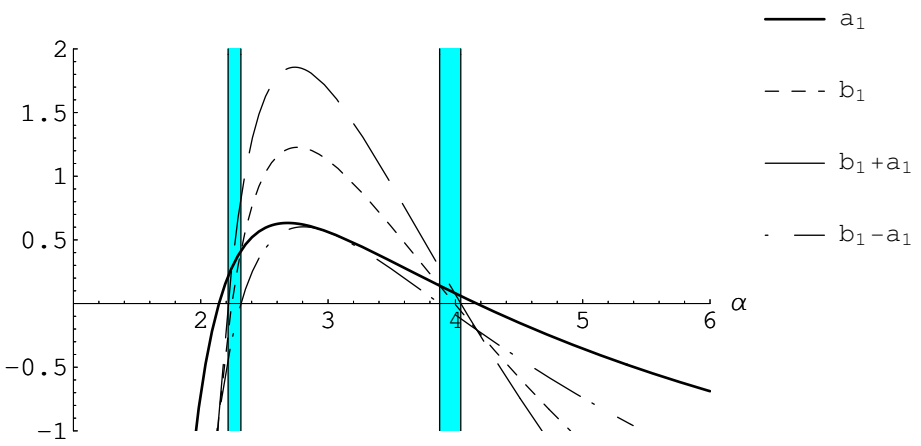

Figure 3.1: Plots of a_1 and b_1, as well as $b_1 \pm a_1$ versus α for $\psi = 30°$

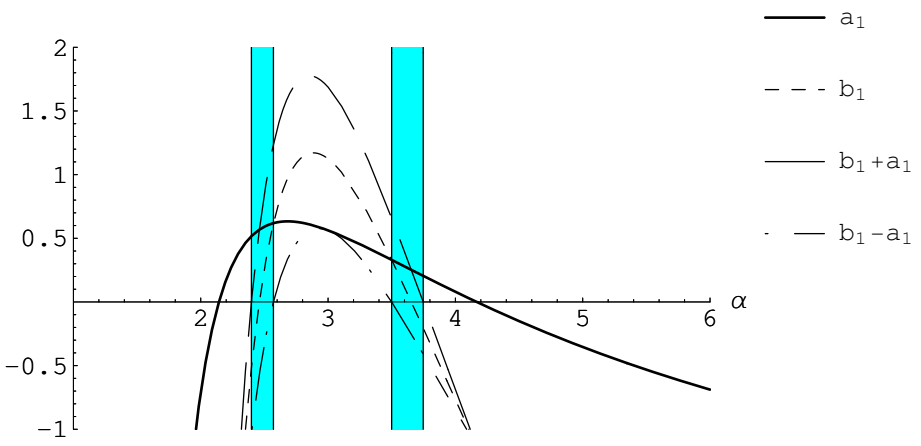

Figure 3.2: Plots of a_1 and b_1, as well as $b_1 \pm a_1$ versus α for $\psi = 45°$

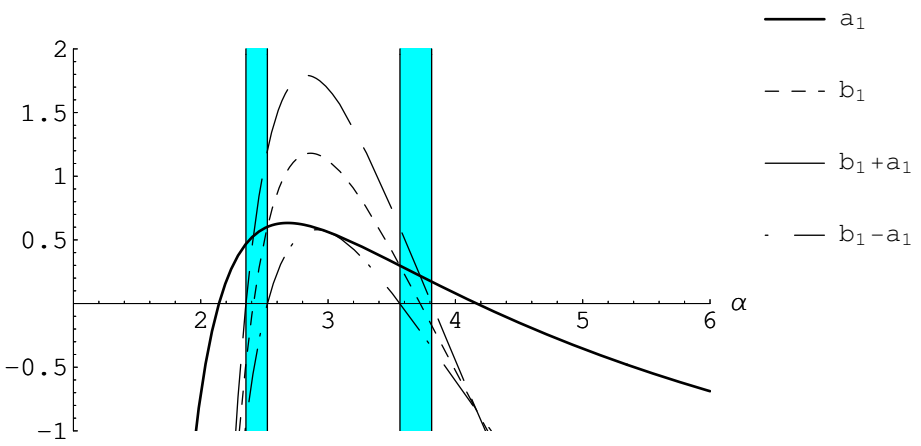

Figure 3.3: Plots of a_1 and b_1, as well as $b_1 \pm a_1$ versus α for $\psi = 75°$

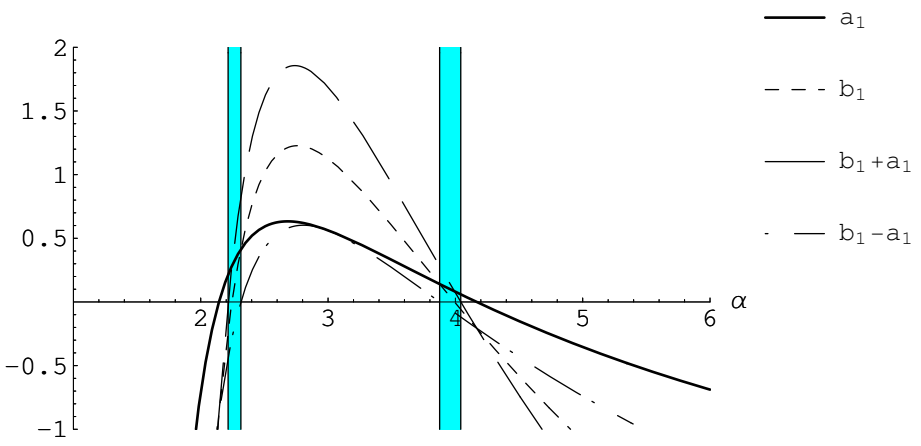

Figure 3.4: Plots of a_1 and b_1, as well as $b_1 \pm a_1$ versus α for $\psi = 90°$

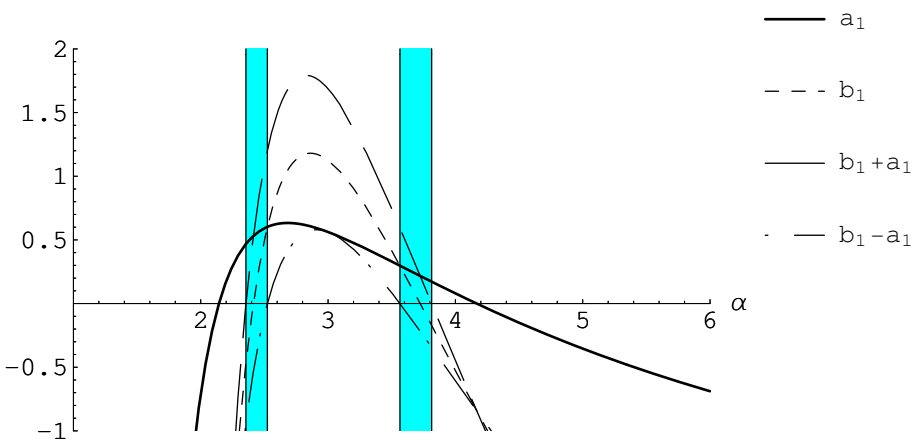

Figure 3.5: Plots of a_1 and b_1, as well as $b_1 \pm a_1$ versus α for $\psi = 105°$

Next we plot our Landau constant stability curves for fixed values of α versus $0 \leq \psi \leq \pi$, with the companion table 3.2. Restricting ourselves to the interval of interest $0 \leq \psi \leq \pi/2$, we see that there are two bands of stable rhombic patterns flanking $\psi/3$, which have again been designated by shading, with no pattern between these bands and stable stripes outside of them. The figures have been drawn for the extended interval $\pi/2 \leq \psi \leq \pi$ in order to demonstrate graphically the symmetry about $\psi = \pi/2$ characteristic of rhombic patterns. We also observe from the figures that there exist no stable rhombic patterns of characteristic angle $\pi/3$ by virtue of the fact that

$$\lim_{\psi \to \pi/3} b_1(\alpha, \psi) \longrightarrow -\infty. \tag{3.9}$$

α	ψ-intervals
2.9	[0.99546, 1.01746], [1.07644, 1.09744], [2.04415, 2.06516], [2.12413, 2.14613]
3.05	[1.02171, 1.03252,], [1.06175, 1.07232], [2.06928, 2.07984], [2.10907, 2.11988]
3.1	[0.99710, 1.01845], [1.07548, 1.09581], [2.04578, 2.06611], [2.12314, 2.14441]
3.2	[0.94668, 0.98946], [1.10308, 1.14228], [1.99931, 2.03851], [2.15213, 2.19491]

Table 3.2: ψ-intervals of stable rhombic patterns for different values of α

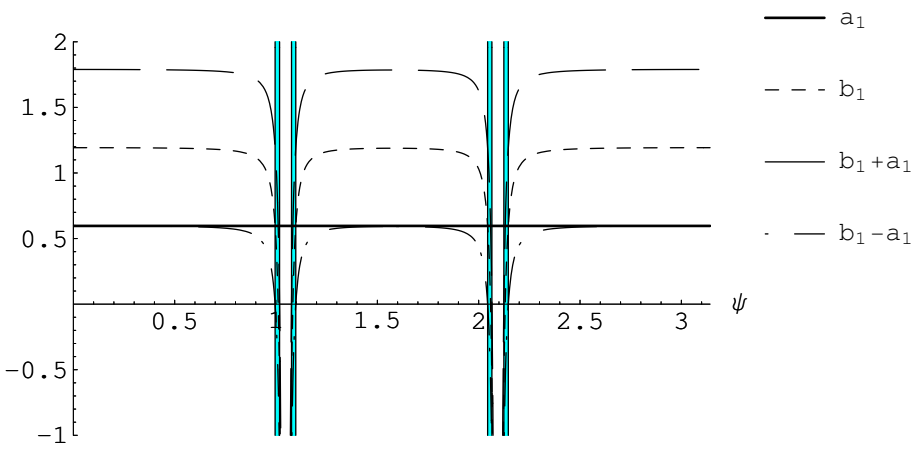

Figure 3.6: Plots of a_1 and b_1, as well as $b_1 \pm a_1$ versus ψ for $\alpha = 2.9$

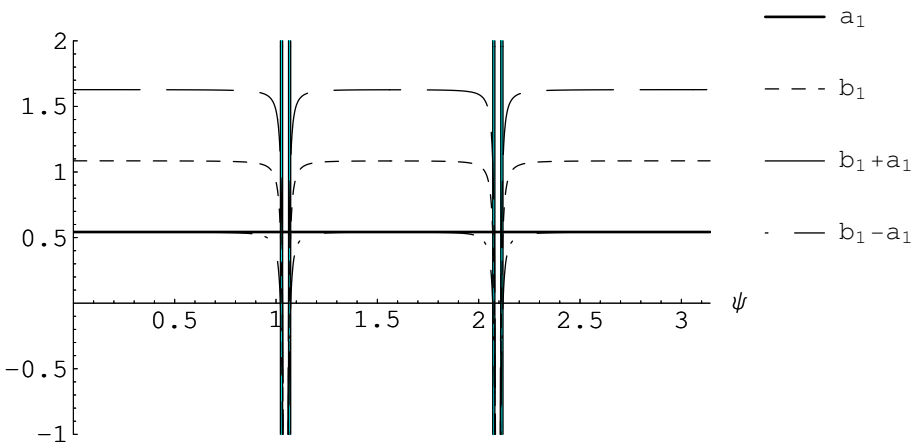

Figure 3.7: Plots of a_1 and b_1, as well as $b_1 \pm a_1$ versus ψ for $\alpha = 3.05$

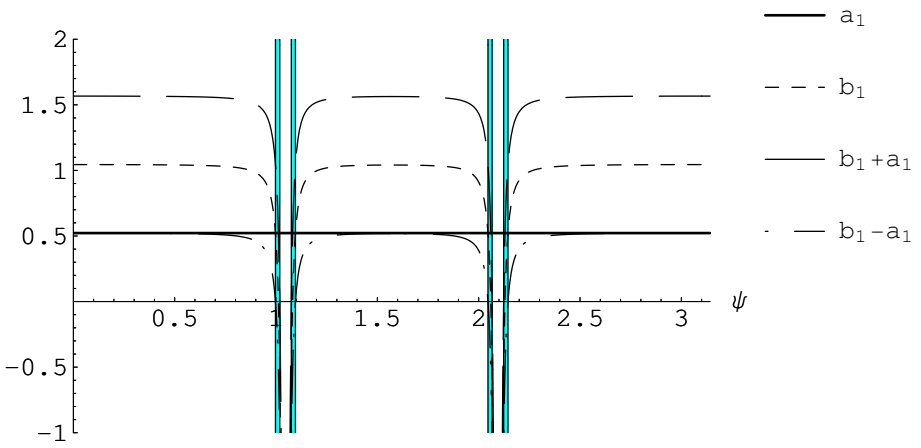

Figure 3.8: Plots of a_1 and b_1, as well as $b_1 \pm a_1$ versus ψ for $\alpha = 3.1$

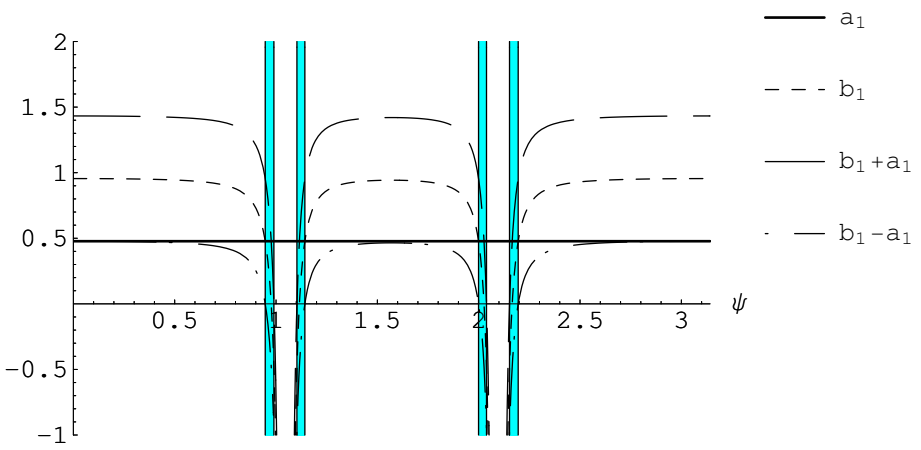

Figure 3.9: Plots of a_1 and b_1, as well as $b_1 \pm a_1$ versus ψ for $\alpha = 3.2$

3.5 Pattern Formation Predictions: An Alternate Approach

The analysis performed in the previous section can be done in a different, and much easier. Motivated by Geddes et al. [4], define the parameter

$$\gamma_1(\alpha, \psi) = \frac{b_1(\alpha, \psi)}{a_1(\alpha)}.$$

Then we see that it is sufficient to have $-1 < \gamma_1 < 1$, since we need $a_1, a_1 + b_1 > 0$ and $b_1 - a_1 < 0$ for $\alpha_1 < \alpha < \alpha_2$ and $0 < \psi \leq \pi/2$. Figures 3.10–3.18 give the same results as figures 3.1–3.9, but using γ_1 instead of a_1 and b_1.

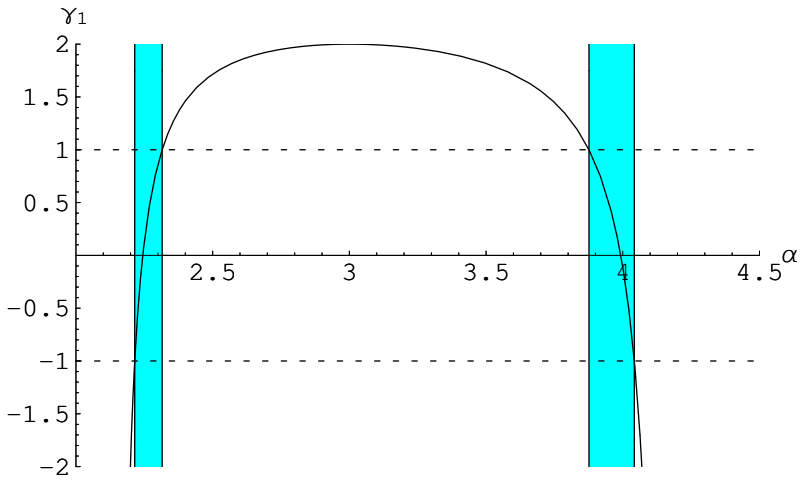

Figure 3.10: Plot of γ_1 versus α for $\psi = 30°$

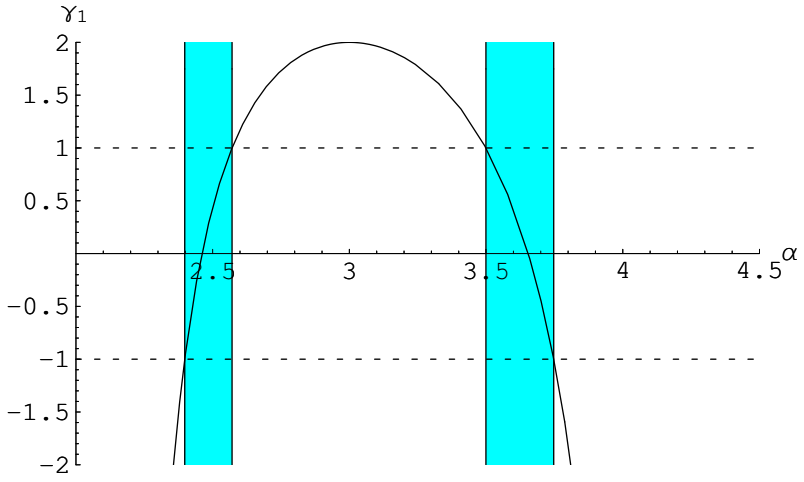

Figure 3.11: Plot of γ_1 versus α for $\psi = 45°$

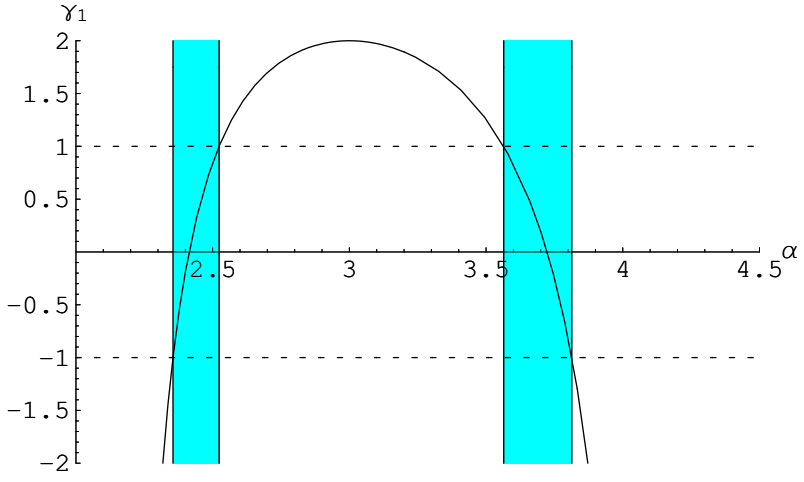

Figure 3.12: Plot of γ_1 versus α for $\psi = 75°$

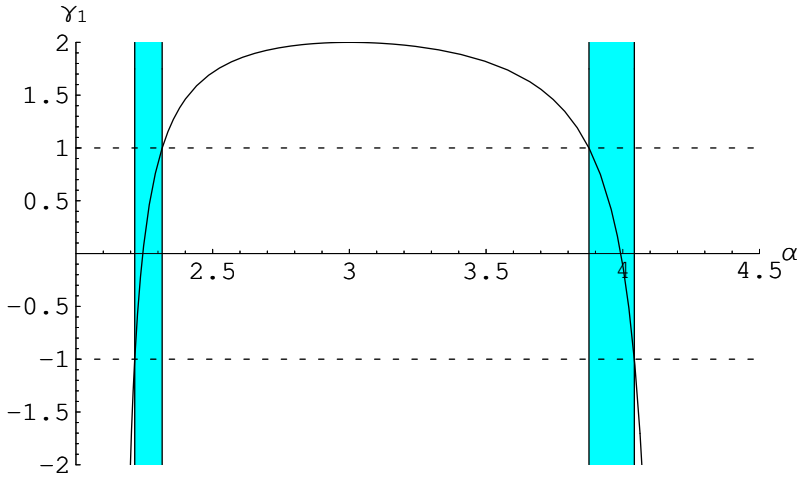

Figure 3.13: Plot of γ_1 versus α for $\psi = 90°$

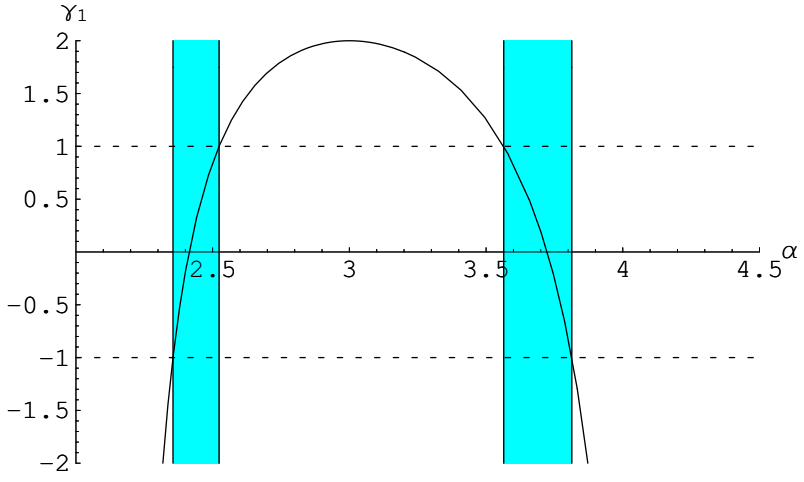

Figure 3.14: Plot of γ_1 versus α for $\psi = 105°$

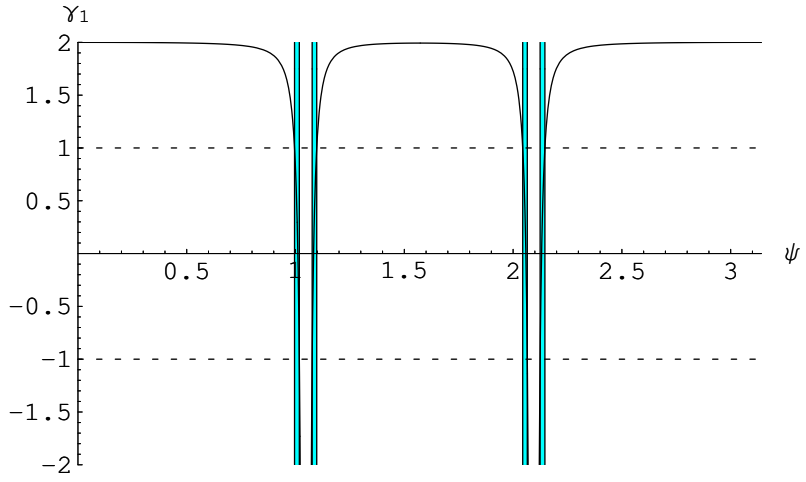

Figure 3.15: Plot of γ_1 versus ψ for $\alpha = 2.9$

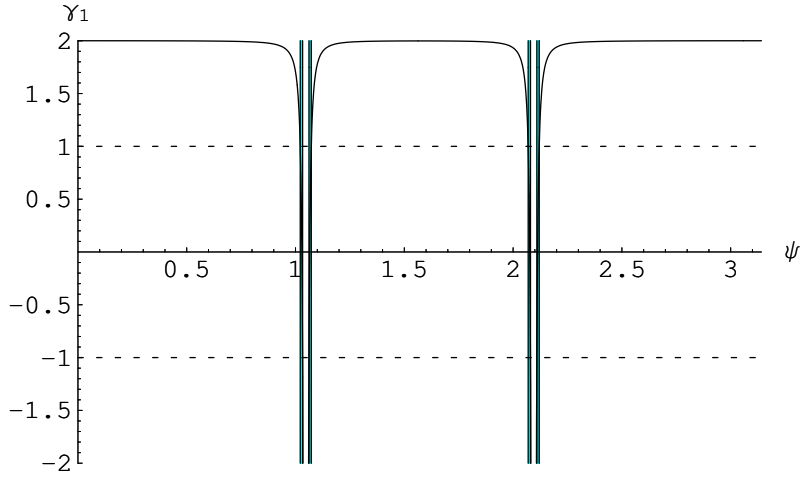

Figure 3.16: Plot of γ_1 versus ψ for $\alpha = 3.05$

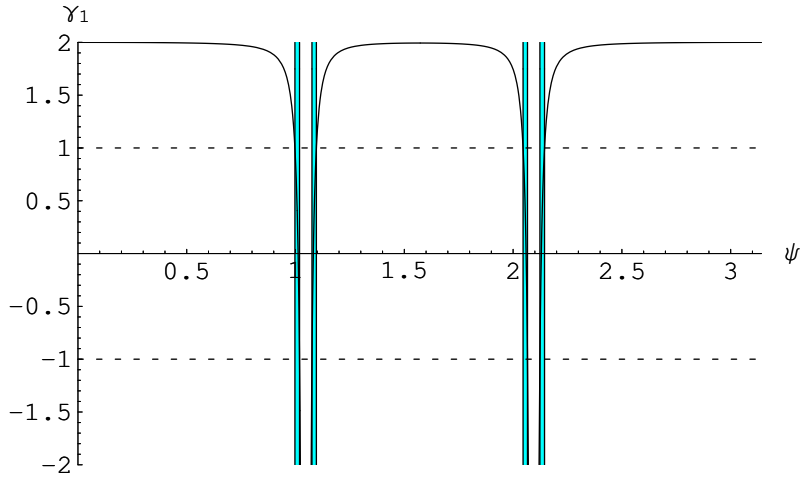

Figure 3.17: Plot of γ_1 versus ψ for $\alpha = 3.1$

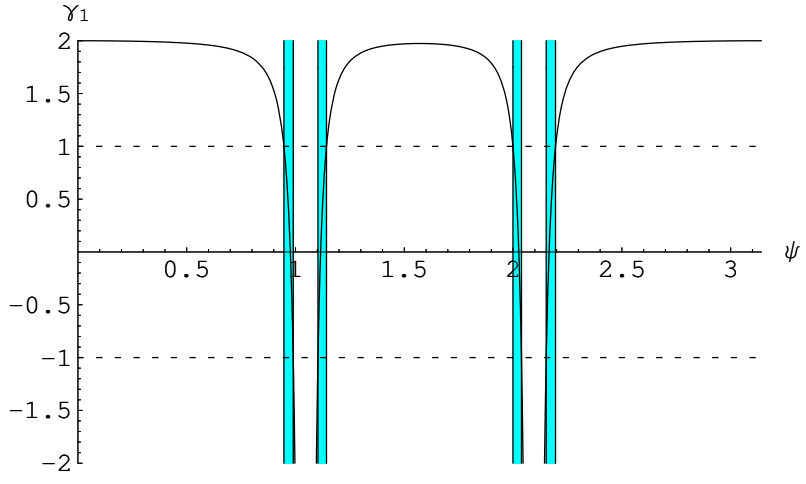

Figure 3.18: Plot of γ_1 versus ψ for $\alpha = 3.2$

3.6 Contour Plots

We close this chapter with a morphological instability interpretation of the potentially stable critical points II and V of our amplitude equations when $\sigma > 0$ relative to the optical patterns under investigation. To lowest order the steady-state equilibrium solution of the governing perturbation evolution equation satisfies

$$\lim_{t\to\infty} R(x,y,t) \sim R_0(x,y) = A_0 \cos(2\pi x/\lambda_c) + B_0 \cos(2\pi z/\lambda_c), \tag{3.10}$$

where $\lambda_c = 2\pi/q_c$.

We represent the contour and density plots for this function with $A_0 > 0$ and $B_0 = 0$ relevant to the critical point II in the x-y plane of figures 3.19 and 3.20. Here the spatial variables are measured in units of λ_c, with elevations appearing light and depressions dark. Clearly such alternating light and dark parallel bands produced by this critical point should be identified with a striped optical pattern as anticipated above. In order to make an analogous interpretation of the critical point V we consider our function R_0 with $B_0 = A_0 > 0$ and allow ψ to take on both some of the values on table 3.1. We represent the contour and density plots for that function with $\psi = 90^\circ$ in figures 3.21 and 3.22. From the checkerboard structure of the latter it is equally clear that this critical point should be identified with an optical pattern of square planform.

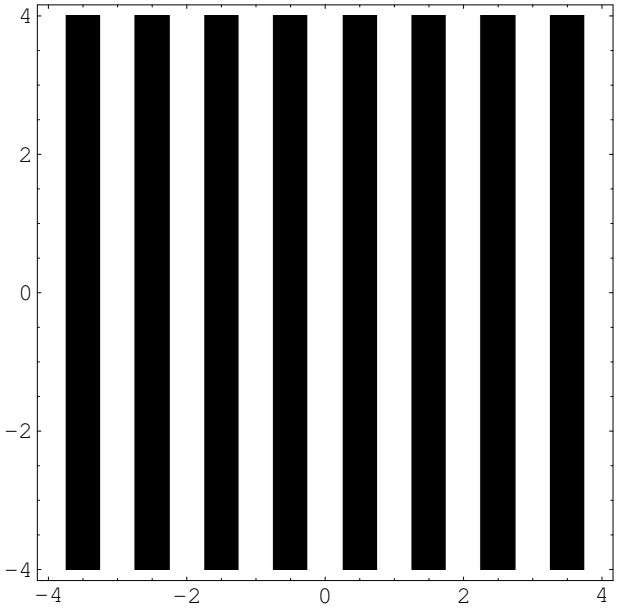

Figure 3.19: Contour plot for critical point II

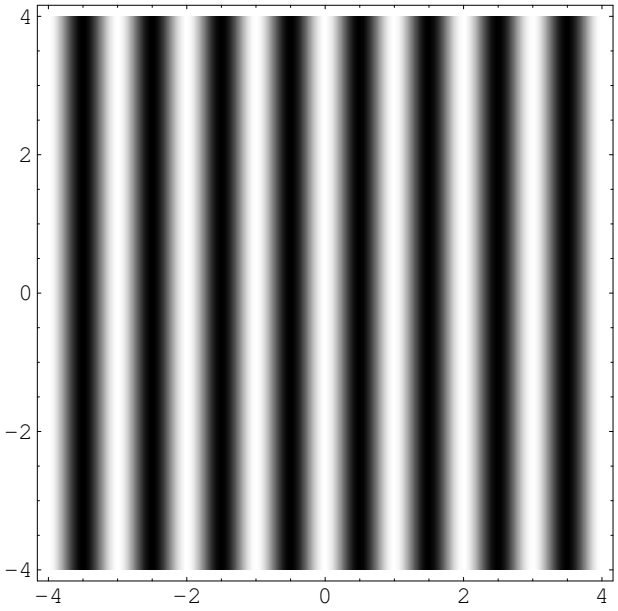

Figure 3.20: Density plot for critical point II

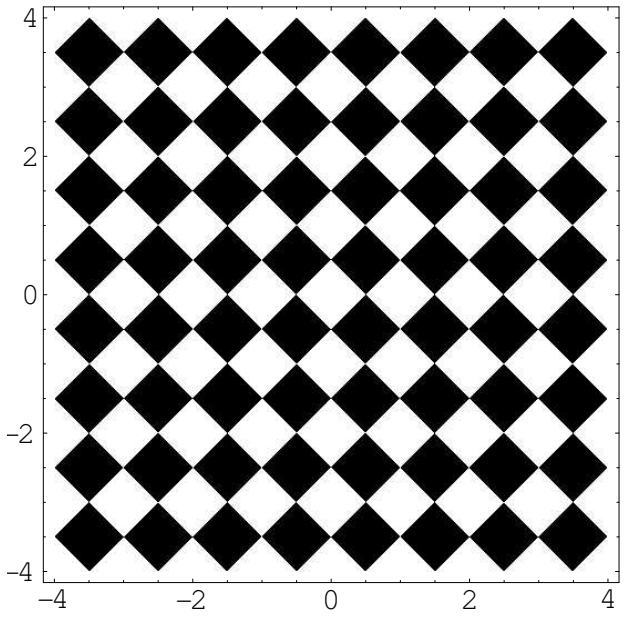

Figure 3.21: Contour plot for critical point V with $\psi = 90°$

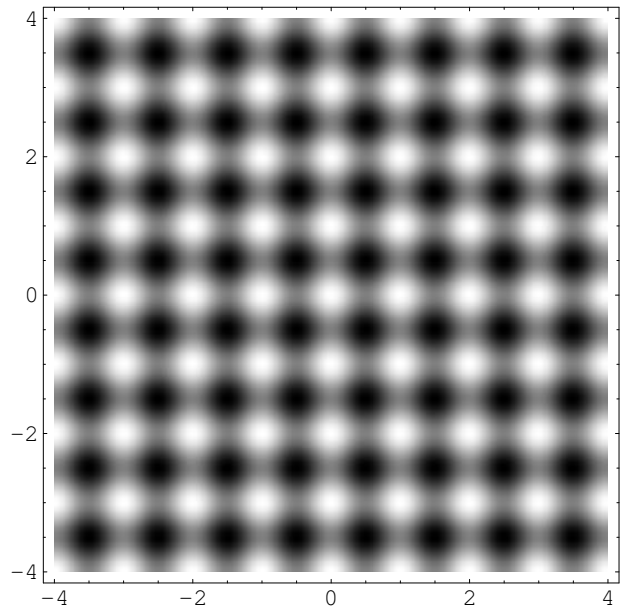

Figure 3.22: Density plot for critical point V with $\psi = 90°$

Finally, in a similar manner we generate the contour plots for other values of ψ, which form a family of rectangles.

To demonstrate this for any ψ, we first put (3.10) for the critical point V in the form

$$R_0(x,y) = A_0\left[\cos(2\pi x/\lambda_c) + \cos(2\pi z/\lambda_c)\right] = 2A_0\cos(\omega_1)\cos(\omega_2), \quad (3.11a)$$

where

$$\omega_1 + \omega_2 = 2\pi x/\lambda_c,\ \omega_1 - \omega_2 = 2\pi z/\lambda_c, \quad (3.11b)$$

or

$$\omega_1 = \pi(x+z)/\lambda_c = (\pi/\lambda_c)\left[\{1+\cos(\psi)\}x + \sin(\psi)y\right], \quad (3.12a)$$

and

$$\omega_2 = \pi(x-z)/\lambda_c = (\pi/\lambda_c)\left[\{1-\cos(\psi)\}x - \sin(\psi)y\right]. \quad (3.12b)$$

From (3.11) and (3.12) we can then deduce that the intersecting level curves in the associated contour plot are two families of straight lines possessing slopes of

$$m_1 = -\left[1+\cos(\psi)\right]/\sin(\psi),\ m_2 = \left[1-\cos(\psi)\right]/\sin(\psi), \quad (3.13a)$$

respectively, which intersect at right angles since

$$m_1 m_2 = -\left[1 - \cos^2(\psi)\right] / \sin^2(\psi) = -\sin^2(\psi) / \sin^2(\psi) = -1. \tag{3.13b}$$

Given that in general this is a rectangular planform we need to explain in what sense such a critical point can be identified with a rhombic pattern. To do so we form the quadrilateral depicted by dashed lines in figure 3.23. Its sides are each composed of two half-diagonals, collectively contained in the four light rectangles surrounding a dark one. Thus, each side of that quadrilateral has the length of one of these diagonals

$$\lambda = \lambda_c / \sin(\psi), \tag{3.14a}$$

where ψ is its characteristic angle $0 < \psi \leq \pi/2$, and hence the quadrilateral is a rhombus. Further, ψ also plays a role in characterizing the family of rectangles. Each member of that family has aspect ratio

$$w/L = \tan(\psi/2), \tag{3.14b}$$

where w and L are its width and length, respectively, while $\psi/2$ serves as its angle of inclination as well, an assertation most easily verified by the

relation

$$\begin{aligned}\tan(\psi/2) &= \left\{\frac{1-\cos(\psi)}{1+\cos(\psi)}\right\}^{1/2} = \left\{\frac{[1-\cos(\psi)]^2}{1-\cos^2(\psi)}\right\}^{1/2} \\ &= \left\{\left[\frac{1-\cos(\psi)}{\sin(\psi)}\right]^2\right\}^{1/2} = \frac{1-\cos(\psi)}{\sin(\psi)} = m_2.\end{aligned} \tag{3.14c}$$

Therefore, we can refer to such an optical pattern as a rhombic array of rectangles.

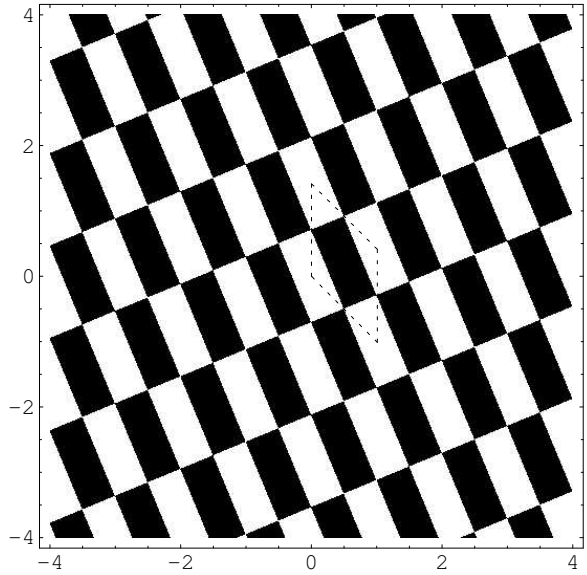

Figure 3.23: Contour plot for critical point V with $\psi = 45°$. Here, the quadrilateral formed by dashed lines depicts the rhombic symmetry of the rectangular pattern

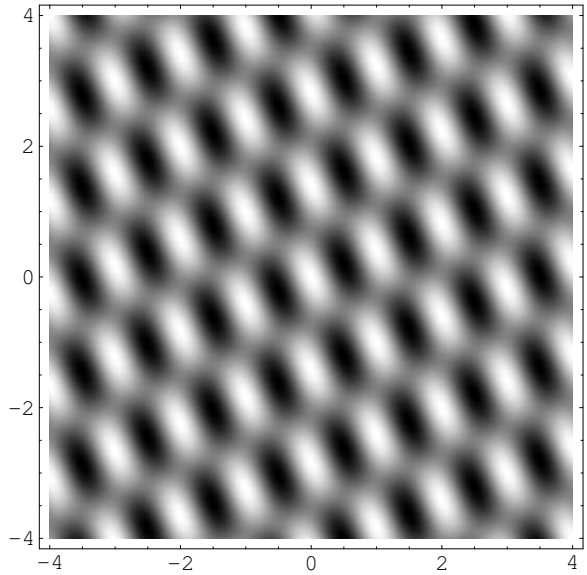

Figure 3.24: Density plot for critical point V with $\psi = 45°$

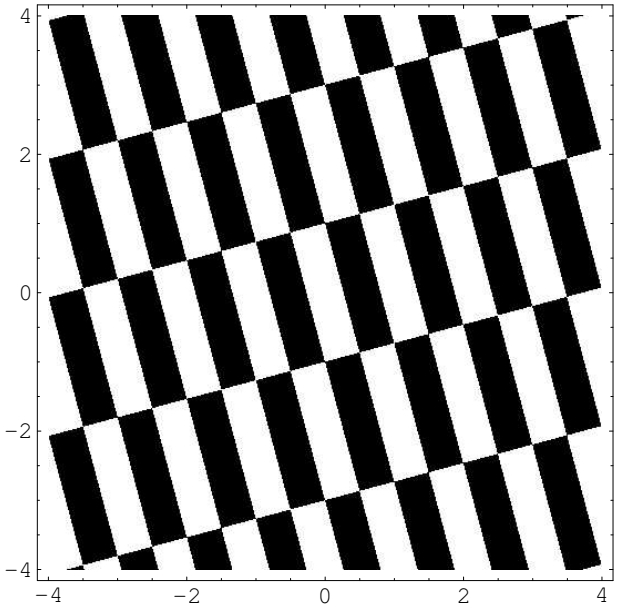

Figure 3.25: Contour plot for critical point V with $\psi = 30°$

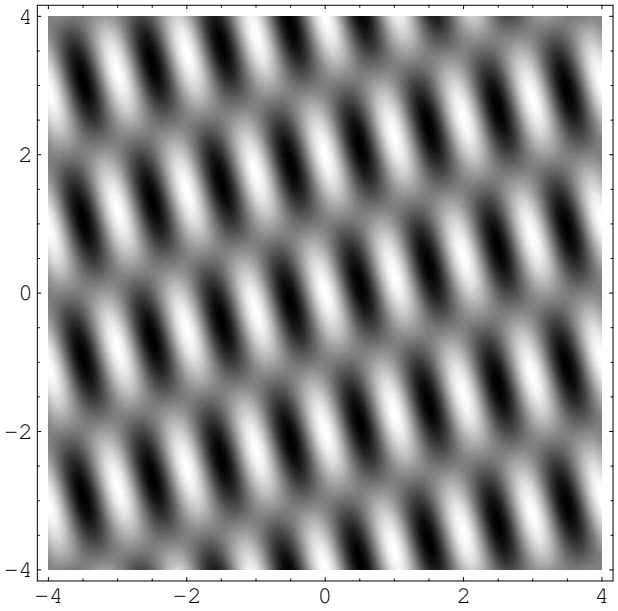

Figure 3.26: Density plot for critical point V with $\psi = 30°$

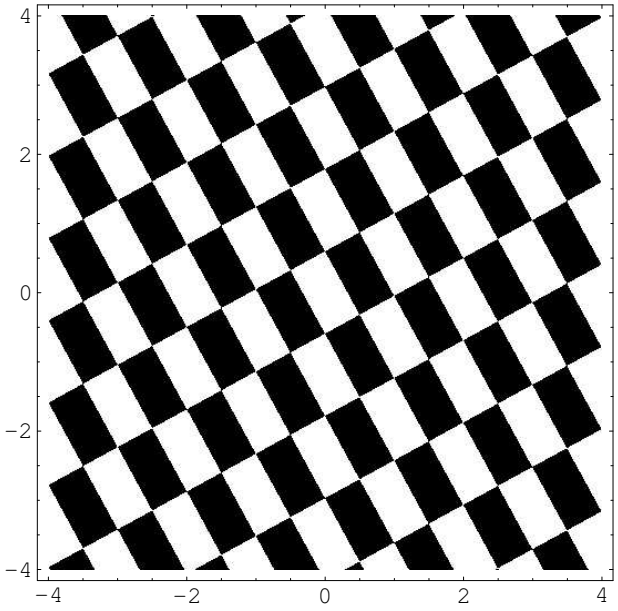

Figure 3.27: Contour plot for critical point V with $\psi = 57°$

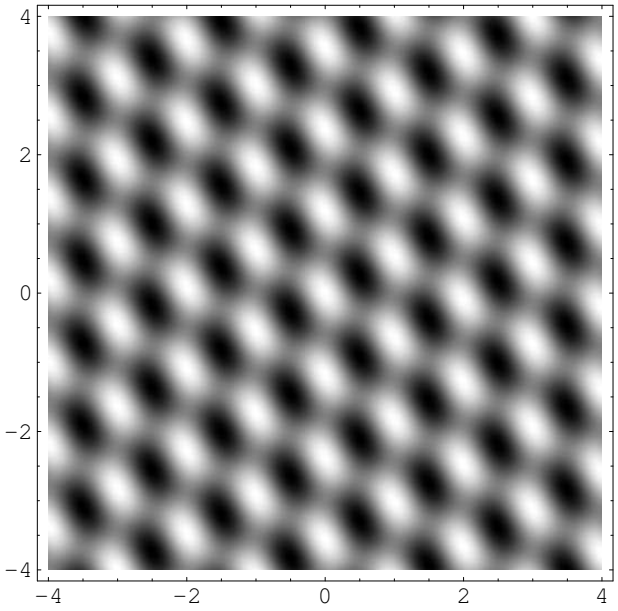

Figure 3.28: Density plot for critical point V with $\psi = 57°$

CHAPTER

FOUR

Discussion

In this dissertation the development of spontaneous stationary equilibrium optical patterns in an atomic sodium vapor ring cavity was investigated by means of a rhombic-planform weakly nonlinear stability analysis applied to equation (2.9), while the hexagonal-planform weakly nonlinear stability analysis was performed by Edmeade [2].

For the rhombic analysis, we sought weakly nonlinear solutions to equation (2.9) which to lowest order satisfy

$$\begin{aligned} R(x,y,t) &\sim A_1(t)\cos(q_c x) + B_1(t)\cos(q_c z), \\ z &= x\cos(\psi) + y\sin(\psi) \end{aligned} \tag{4.1a}$$

such that

$$\begin{aligned} \frac{\mathrm{d}A_1}{\mathrm{d}t} &\sim \sigma A_1 - A_1(a_1 A_1^2 + b_1 B_1^2), \\ \frac{\mathrm{d}B_1}{\mathrm{d}t} &\sim \sigma B_1 - B_1(b_1 A_1^2 + a_1 B_1^2), \end{aligned} \tag{4.1b}$$

while for the hexagonal one (see [2, 8]), the solution satisfies

$$\begin{aligned} R(x,y,t) \sim\ & A_1(t)\cos[q_c x + \phi_1(t)] + \\ & + A_2(t)\cos\left[\tfrac{1}{2}q_c(x - \sqrt{3}y) - \phi_2(t)\right] + \\ & + A_3(t)\cos\left[\tfrac{1}{2}q_c(x + \sqrt{3}y) - \phi_3(t)\right], \end{aligned} \tag{4.2a}$$

where

$$\frac{\mathrm{d}A_i}{\mathrm{d}t} \sim \sigma A_i - 4a_0 A_j A_k \cos(\phi_i + \phi_j + \phi_k) - A_i\left[a_1 A_i^2 + 2a_2(A_j^2 + A_k^2)\right], \tag{4.2b}$$

$$\begin{aligned} A_i \frac{\mathrm{d}\phi_i}{\mathrm{d}t} &\sim 4a_0 A_j A_k \sin(\phi_i + \phi_j + \phi_k), \\ (i,j,k) &= \text{even permutation of } (1,2,3). \end{aligned} \tag{4.2c}$$

Our analysis of section 3.3 shows that equations (4.1b) possess the following equivalence classes of critical points: I : $A_0 = B_0 = 0$; II : $A_0^2 = \sigma/a_1$, $B_0 = 0$; V : $A_0 = B_0$, with $A_0^2 = \sigma/(a_1 + b_1)$. Assuming that $a_1, a_1 + b_1 > 0$, we investigated the stability of these critical points and found that I is stable for $\sigma < 0$; II, for $\sigma > 0$, $b_1 > a_1$; and V, for $\sigma > 0$, $a_1 > b_1$. Equivalence classes I and II represent the undisturbed and striped states, respectively, while V can be identified with a rhombic array of

rectangles of characteristic angle ψ (see section 3.6). We used these criteria to find α-intervals where rhombic patterns arise. Toward this end, we examined the signs of $a_1 + b_1$ and $b_1 - a_1$ for $\alpha_1 < \alpha < \alpha_2$ and $0 < \psi \leq \pi/2$, with $\pi/2$ (or equivalently 90°) representing a square planform, using the explicit formulae for a_1 and b_1 given by equations (3.4) and (3.5). Tables 3.1 and 3.2, together with figures 3.1–3.9 summarize our results. We see in these figures that for a fixed value of alpha there are two narrow bands of stable rhombic patterns flanking $\psi = \pi/3$ with no pattern between these bands and stable stripes outside them. There exist no stable rhombic patterns of characteristic angle $\pi/3$. Wollkind and Stephenson [15] conjectured that this angle was reserved for hexagonal arrays.

For the sake of completeness, we include here a summary of the results of Edmeade [2]. In cataloguing the critical points of (4.2b,c), and summarizing their orbital stability behaviour it is necessary to employ the quantities

$$\begin{gathered} \sigma_{-1} = -4a_0^2/(a_1 + 4a_2), \quad \sigma_1 = 16a_1a_0^2/(2a_2 - a_1)^2, \\ \sigma_2 = 32(a_1 + a_2)a_0^2/(2a_2 - a_1)^2. \end{gathered} \tag{4.3}$$

There exist equivalence classes of (4.2b,c) given by $\phi_1 = \phi_2 = \phi_3 = 0$ and I : $A_1 = A_2 = A_3 = 0$; II : $A_1^2 = \sigma/a_1$, $A_2 = A_3 = 0$; III$^{\pm}$: $A_1 = A_2 = A_3 = A_0^{\pm} = \{-2a_0 \pm [4a_0^2 + (a_1 + 4a_2)\sigma]^{1/2}\}/(a_1 + 4a_2)$; IV : $A_1 = -4a_0/(2a_2 - a_1)$, $A_2^2 = A_3^2 = (\sigma - \sigma_1)/(a_1 + 2a_2)$; where it is assumed that $a_1, a_1 + 4a_2 > 0$. The orbital stability conditions for these critical points can be posed in terms

a_0	$2a_2 - a_1$	Stable Structures
$+$	$-, 0$	III^- for $\sigma > \sigma_{-1}$
$+$	$+$	III^- for $\sigma_{-1} < \sigma < \sigma_2$, II for $\sigma > \sigma_1$
0	$-$	$\mathrm{III}^\pm$ for $\sigma > 0$
0	$+$	II for $\sigma > 0$
$-$	$+$	III^+ for $\sigma_{-1} < \sigma < \sigma_2$, II for $\sigma > \sigma_1$
$-$	$-, 0$	III^+ for $\sigma > \sigma_{-1}$

Table 4.1: Orbital stability behavior of critical points II and $\mathrm{III}^\pm$

of σ. Thus critical point I is stable in this sense for $\sigma < 0$ while the stability behavior of II and $\mathrm{III}^\pm$ which depends upon the signs of a_0 and $2a_2 - a_1$ as well has been summarized in table 4.1. Here, when stable, II and $\mathrm{III}^\pm$ represent one- and two-dimensional periodic structures, respectively, the latter pattern exhibiting hexagonal symmetry in the plane such that $A_0^+ > 0$ and $A_0^- < 0$. Finally, critical point IV, which reduces to II for $\sigma = \sigma_1$ and to $\mathrm{III}^\pm$ for $\sigma = \sigma_2$ and hence called a generalized cell, is not stable for any value of σ. For our problem (see [2]), critical points I and II represent the undisturbed state and the supercritical state of stripe patterns, respectively, while critical point III^+ can be identified with hexagonal arrays of dots or bright spots, and III^- with hexagonal arrays of nets or honeycombs (see figures 4.2–4.5).

In order to compare these theoretical results with experimental observation and numerical simulations, Edmeade [2] represented the results of table 4.1 graphically in the α-β plane. There exists a critical value that

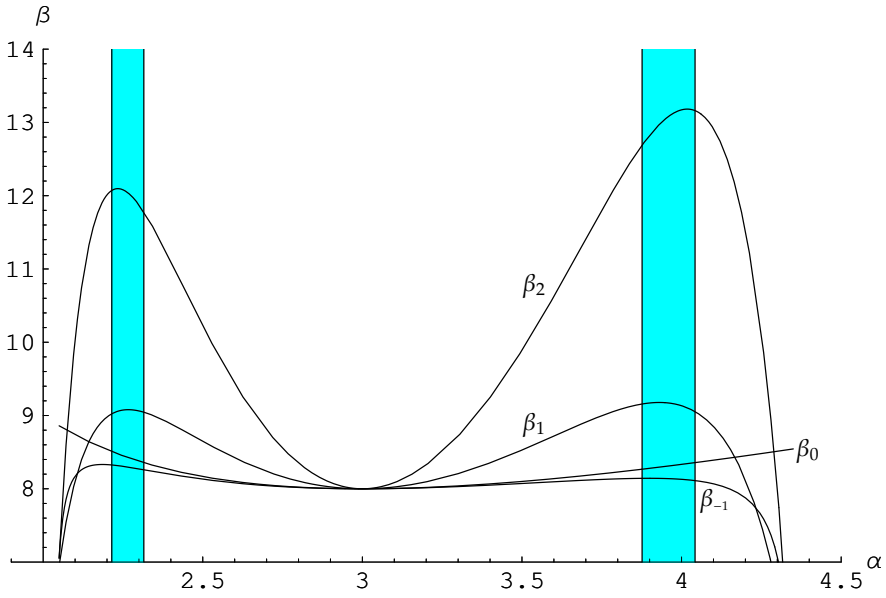

Figure 4.1: Plots of β_i versus α, for $i = -1, 0, 1, 2$. The shaded regions indicate the α-intervals where square patterns may arise

satisfies the conditions

$$a_0 = 0 \text{ for } \alpha = \alpha_c, \tag{4.4a}$$

$$a_0 < 0 \text{ for } \alpha < \alpha_c, \tag{4.4b}$$

$$a_0 > 0 \text{ for } \alpha > \alpha_c. \tag{4.4c}$$

This value was determined to be $\alpha_c = 3$. In addition, Edmeade [2] defined the quantities

$$\beta_i = \beta_0(\sigma_i + 1) \tag{4.5}$$

for $i = -1, 0, 1, 2$. Graphs of $\beta_i(\alpha)$, for $i = -1, 0, 1, 2$, are shown in figure 4.1. As usual, α represents the square of the magnitude of the intracavity

field and β represents the absorption coefficient. From equations (4.4), table 4.1 and figure 4.1 we can deduce that stripes form for $\alpha = \alpha_c = 3$, honeycombs for $\alpha < \alpha_c$, and spots for $\alpha > \alpha_c$, which is consistent with the results of Firth and Scroggie [3].

In addition, the regions of the α-β plane where stable square patterns may arise is denoted by shading. According to Edmeade [2], hexagons and stripes may coexist when $\beta_1 < \beta < \beta_2$, and stripes alone exist for $\beta > \beta_2$. Firth and Scroggie [3] did not observe this coexistence with their numerical simulations. This is because the regions of coexistence fall in the shaded region where square patterns arise. In this region stripes cannot exist at all, since they are unstable with respect to squares, unless $\alpha = \alpha_c$, where β_0 attains its minimum. For this value of α neither hexagons nor rhombi can exist, but for $\alpha \approx \alpha_c$, the region where hexagonal patterns form is very small, and thus rhombic patterns dominate. However for these values of α (see table 3.1), $\psi \approx \pi/3$, and so the rhombic pattern resembles a hexagonal one.

Another feature of our stability analysis is that it shows that patterns saturate at cubic order, even though Geddes et al. [4] insist that these patterns saturate at quintic order. Their problem is not the same as ours, but it is similar. They obtained square and hexagonal patterns with their numerical simulations, although these numerical results do not agree with their analytic results. We, on the other hand, obtained such patterns analytically, and our weak solution (3.1) can be used in numerical simulations to generate rhombic-patterns.

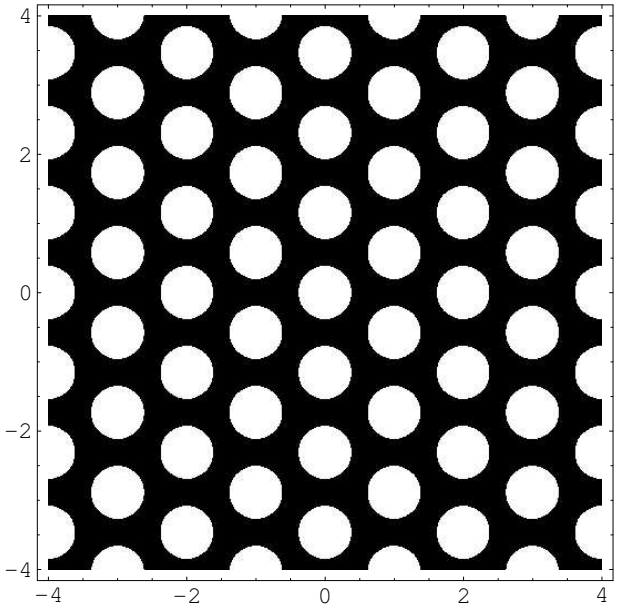

Figure 4.2: Contour plot for critical point III^{+}

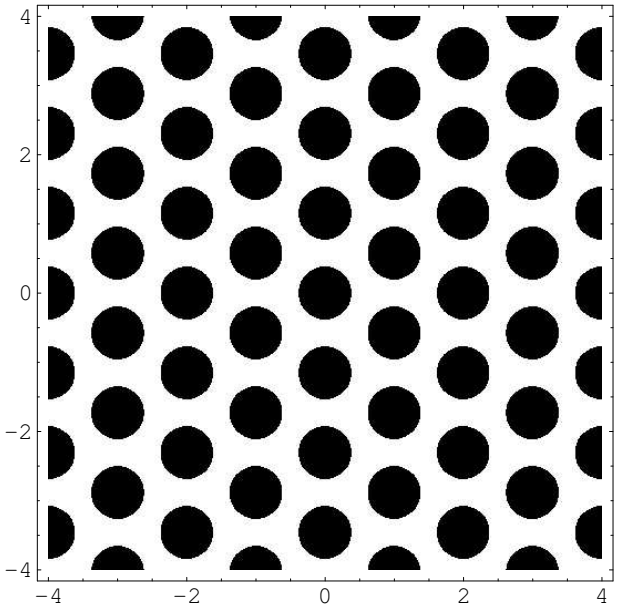

Figure 4.3: Contour plot for critical point III^{-}

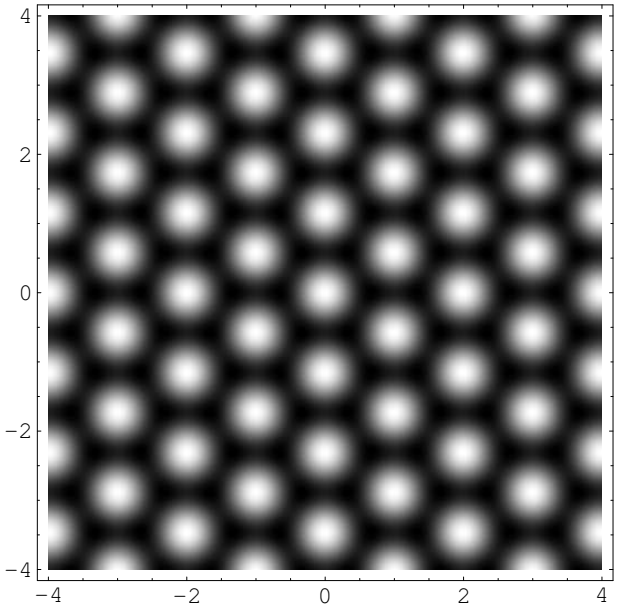

Figure 4.4: Density plot for critical point III^{+}

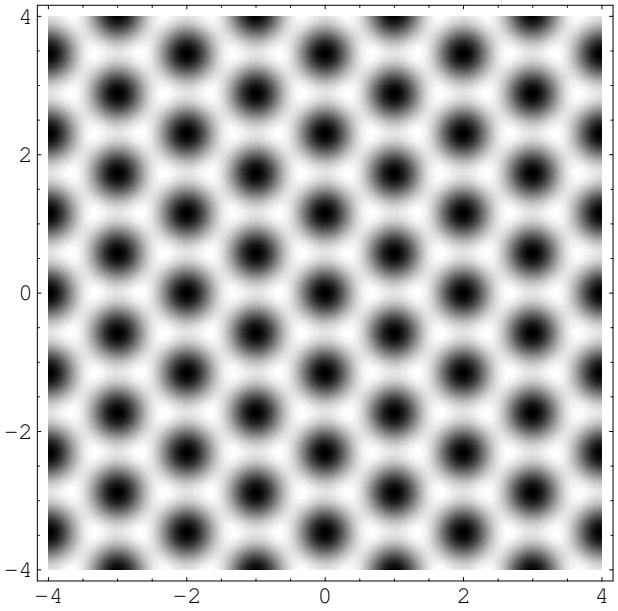

Figure 4.5: Density plot for critical point III^{-}

CHAPTER

FIVE

Appendices

A Derivation of the Two-Level Kerr-Cavity Equation

Consider the Maxwel-Bloch equations

$$X_t = -(1 + \mathrm{i}\theta)X + Y - \beta P + \mathrm{i}\chi\nabla^2 X, \tag{A.1}$$

$$\varepsilon_1 P_t = fX - (1 + \mathrm{i}\Delta)P, \tag{A.2}$$

$$\varepsilon_2 f_t = 1 - f - \tfrac{1}{2}(X^* P + X P^*). \tag{A.3}$$

Letting $\varepsilon_{1,2} \to 0$ we obtain

$$P = \frac{fX}{1 + \mathrm{i}\Delta} \tag{A.4}$$

$$f = 1 - \mathrm{Re}(X^* P). \tag{A.5}$$

Substituting equation (A.4) into equation (A.5) yields

$$f = 1 - \frac{f\,|X|^2}{1 + \Delta^2},$$

and solving for f we obtain

$$f = \frac{1 + \Delta^2}{1 + \Delta^2 + |X|^2}. \tag{A.6}$$

Substituting equation (A.6) into equation (A.4) gives the quasi-equilibrium

conditions

$$f = \frac{1 + \Delta^2}{1 + \Delta^2 + |X|^2} \tag{A.7}$$

$$P = \frac{(1 - \mathrm{i}\Delta)X}{1 + \Delta^2 + |X|^2}, \tag{A.8}$$

Substituting equations (A.8) into equation (A.1) reduces the system to the single model equation in X given by

$$X_t = -X\left[1 + \mathrm{i}\theta + \frac{\beta(1 - \mathrm{i}\Delta)}{1 + \Delta^2 + |X|^2}\right] + Y + \mathrm{i}\chi\nabla^2 X. \tag{A.9}$$

B Derivation of β_{crit}

Consider the following

$$X_t = -X\left[1 + \mathrm{i}\theta + \frac{\beta(1 - \mathrm{i}\Delta)}{1 + \Delta^2 + |X|^2}\right] + Y + \mathrm{i}\chi\nabla^2 X. \tag{B.1}$$

Let $X \equiv X_0$ be a constant solution to equation (B.1). We have, then,

$$Y = X_0\left[\left(1 + \frac{\beta}{1 + \Delta^2 + |X|^2}\right) + \mathrm{i}\left(\theta - \frac{\beta\Delta}{1 + \Delta^2 + |X|^2}\right)\right],$$

and so $|Y|^2 = YY^*$ yields

$$Y^2 = \alpha\left[\left(1 + \frac{\beta}{\mathcal{D}}\right)^2 + \left(\theta - \frac{\beta\Delta}{\mathcal{D}}\right)^2\right], \tag{B.2}$$

where $\alpha = |X_0|^2$, $\mathcal{D} = 1 + \Delta^2 + \alpha$ and assuming $Y \in \mathbb{R}$ (see [7]).

Multiplying equation (B.2) by $\mathcal{D}^2$ we obtain

$$\begin{aligned}\mathcal{D}^2Y^2 &= \alpha[(\mathcal{D} + \beta)^2 + (\theta\mathcal{D} - \beta\Delta)^2] \\ &= \alpha[(1 + \theta^2)\mathcal{D}^2 + 2\beta(1 - \Delta\theta)\mathcal{D} + (1 + \Delta^2)\beta^2],\end{aligned}$$

and hence

$$Y^2 = \alpha\left[(1 + \theta^2) + \frac{2\beta(1 - \Delta\theta)}{\mathcal{D}} + \frac{\beta^2(1 + \Delta^2)}{\mathcal{D}^2}\right].$$

Making use of the following:

$$\frac{\mathrm{d}}{\mathrm{d}\alpha}\left(\frac{\alpha}{\mathcal{D}}\right) = \frac{\mathcal{D} - \alpha\mathcal{D}'}{\mathcal{D}^2} = \frac{1+\Delta^2}{\mathcal{D}^2}$$

$$\frac{\mathrm{d}}{\mathrm{d}\alpha}\left(\frac{\alpha}{\mathcal{D}^2}\right) = \frac{\mathcal{D}^2 - 2\alpha\mathcal{D}\mathcal{D}'}{\mathcal{D}^4} = \frac{1+\Delta^2-\alpha}{\mathcal{D}^3}$$

we obtain

$$\frac{\mathrm{d}\Upsilon^2}{\mathrm{d}\alpha} = (1+\theta^2) + \frac{2\beta(1-\Delta\theta)(1+\Delta^2)}{\mathcal{D}^2} + \frac{\beta^2(1+\Delta^2-\alpha)(1+\Delta^2)}{\mathcal{D}^3}$$

or

$$\mathcal{D}^3\frac{\mathrm{d}\Upsilon^2}{\mathrm{d}\alpha} = (1+\theta^2)\mathcal{D}^3 + 2\beta(1-\Delta\theta)(1+\Delta^2)\mathcal{D} + \beta^2(1+\Delta^2-\alpha)(1+\Delta^2). \tag{B.3}$$

We now focus on the right-hand side of equation (B.3). Substituting $-\alpha = 1 + \Delta^2 - \mathcal{D}$ into equation (B.3) we obtain

$$(1+\theta^2)\mathcal{D}^3 + [2\beta(1-\Delta\theta) - \beta^2](1+\Delta^2)\mathcal{D} + 2\beta^2(1+\Delta^2)^2 = 0$$

for $\beta = \beta_{crit}$.

Following the method of Uspensky [12], consider $z^3 + bz + c = 0$ and $4b^3 + 27c^2 = 0$, where

$$b = \left(\frac{1+\Delta^2}{1+\theta^2}\right)[2\beta(1-\Delta\theta) - \beta^2],$$

and

$$c = \frac{2\beta^2(1+\Delta^2)^2}{1+\theta^2}.$$

Then

$$\begin{aligned} 4b^3 + 27c^2 &= 4\beta^3\left(\frac{1+\Delta^2}{1+\theta^2}\right)^3[2(1-\Delta\theta) - \beta]^3 + 27 \cdot \frac{4\beta^4(1+\Delta^2)^4}{(1+\theta^2)^2} \\ &= 4\beta^3\left(\frac{1+\Delta^2}{1+\theta^2}\right)^3[27\beta(1+\Delta^2)(1+\theta^2) - (\beta - 2(1-\Delta\theta))^3]. \end{aligned}$$

Therefore,

$$4b^3 + 27c^2 = 0$$

if and only if

$$27\beta(1+\Delta^2)(1+\theta^2) = (\beta - 2(1-\Delta\theta))^3,$$

which is satisfied for $\beta = \beta_{crit}$. Thus, β_{crit} is defined implicitly by

$$27\beta_{crit}(1+\Delta^2)(1+\theta^2) = (\beta_{crit} - 2(1-\Delta\theta))^3.$$

C Linear Stability Analysis

Consider the Maxwell-Bloch equations (A.1)–(A.3), and let $X \equiv X_0, P \equiv P_0$ and $f \equiv f_0$ be constant solutions. From equation (A.1),

$$0 = -(1 + \mathrm{i}\theta)X_0 + Y - \beta P_0,$$

since $X_t = \nabla^2 X = 0$. Then

$$Y_0 = (1 + \mathrm{i}\theta)X_0 + \beta P_0. \tag{C.1}$$

From equations (A.2)–(A.3),

$$0 = f_0 X_0 - (1 + \mathrm{i}\Delta)P_0$$
$$0 = 1 - f_0 - \tfrac{1}{2}(X_0^* P_0 + X_0 P_0^*) = 1 - f_0 - \mathrm{Re}(X_0^* P_0).$$

Solving for $\{f_0, P_0\}$:

$$P_0 = \frac{f_0 X_0}{1 + \mathrm{i}\Delta} \tag{C.2}$$
$$f_0 = 1 - \mathrm{Re}(X_0^* P_0). \tag{C.3}$$

Substituting (C.2) into (C.3):

$$f_0 = 1 - \mathrm{Re}\left(X_0^* \frac{f_0 X_0}{1 + \mathrm{i}\Delta}\right) = 1 - \mathrm{Re}\left(\frac{f_0 |X_0|^2 (1 - \mathrm{i}\Delta)}{1 + \Delta^2}\right)$$
$$= 1 - \frac{f_0 |X_0|^2}{1 + \Delta^2},$$

and solving this equation for f_0 we obtain

$$f_0\left(1 + \frac{|X_0|^2}{1 + \Delta^2}\right) = f_0\left(\frac{1 + \Delta^2 + |X_0|^2}{1 + \Delta^2}\right) = 1$$

or

$$f_0 = \frac{1 + \Delta^2}{1 + \Delta^2 + |X_0|^2} = \frac{1 + \Delta^2}{\mathcal{D}}, \quad \text{where } \mathcal{D} = 1 + \Delta^2 + \alpha,\ \alpha = |X_0|^2,$$

and substituting into (C.2),

$$P_0 = \frac{(1 + \Delta^2)X_0}{(1 + \mathrm{i}\Delta)\mathcal{D}} = \frac{(1 + \Delta^2)X_0}{(1 + \mathrm{i}\Delta)\mathcal{D}} \cdot \frac{1 - \mathrm{i}\Delta}{1 - \mathrm{i}\Delta},$$

i.e.,

$$P_0 = \frac{(1 - \mathrm{i}\Delta)X_0}{\mathcal{D}}.$$

Now, let

$$X = X_0(1 + A), \quad P = P_0(1 + B), \quad f = f_0(1 + C).$$

Thus, from (A.1) and (C.1),

$$\begin{aligned} X_0 A_t &= -(1 + \mathrm{i}\theta)X_0(1 + A) + (1 + \mathrm{i}\theta)X_0 + \beta P_0 - \beta P_0(1 + B) + \mathrm{i}\chi X_0 \nabla^2 A \\ &= -(1 + \mathrm{i}\theta)X_0 A - \beta P_0 B + \mathrm{i}\chi X_0 \nabla^2 A \\ &= -(1 + \mathrm{i}\theta)X_0 A - \beta \frac{(1 - \mathrm{i}\Delta)X_0}{\mathcal{D}} B + \mathrm{i}\chi X_0 \nabla^2 A, \end{aligned}$$

or

$$A_t = -(1 + \mathrm{i}\theta)A - \beta \frac{(1 - \mathrm{i}\Delta)}{\mathcal{D}} B + \mathrm{i}\chi \nabla^2 A. \tag{C.4}$$

From (A.2)

$$\begin{aligned} \varepsilon_1 P_0 B_t &= f_0(1 + C)X_0(1 + A) - (1 + \mathrm{i}\Delta)P_0(1 + B) \\ &= (1 + \mathrm{i}\Delta)P_0(1 + C)(1 + A) - (1 + \mathrm{i}\Delta)P_0(1 + B) \\ &= (1 + \mathrm{i}\Delta)P_0(1 + A + C + AC - 1 - B) \end{aligned}$$

or

$$\varepsilon_1 B_t = (1 + \mathrm{i}\Delta)(A + C + AC - B). \tag{C.5}$$

From (A.3)

$$\begin{aligned}\varepsilon_2 f_0 C_t &= 1 - f_0(1+C) - \tfrac{1}{2}X_0^* P_0(1+A^*)(1+B) - \tfrac{1}{2}X_0 P_0^*(1+A)(1+B^*) \\ &= 1 - f_0 - f_0 C - \tfrac{1}{2}X_0^* \frac{(1-\mathrm{i}\Delta)}{\mathcal{D}} X_0(1+A^*)(1+B) + \\ &\qquad - \tfrac{1}{2}X_0 \frac{(1+\mathrm{i}\Delta)}{\mathcal{D}} X_0^*(1+A)(1+B^*)\end{aligned}$$

or

$$\begin{aligned}&\varepsilon_2 \frac{1+\Delta^2}{\mathcal{D}} C_t = \\ &= \frac{\alpha}{\mathcal{D}} - \frac{1+\Delta^2}{\mathcal{D}} C - \frac{(1-\mathrm{i}\Delta)}{2\mathcal{D}}\alpha(1+A^*+B+A^*B) - \frac{(1+\mathrm{i}\Delta)}{2\mathcal{D}}\alpha(1+A+B^*+AB^*),\end{aligned}$$

i.e.,

$$\varepsilon_2(1+\Delta^2)C_t = -(1+\Delta^2)C - \tfrac{1}{2}(1-\mathrm{i}\Delta)\alpha(A^*+B+A^*B) - \tfrac{1}{2}(1+\mathrm{i}\Delta)\alpha(A+B^*+AB^*). \tag{C.6}$$

We have, then, that

$$\begin{aligned}A_t &= -(1+\mathrm{i}\theta)A - \beta\frac{(1-\mathrm{i}\Delta)}{\mathcal{D}}B + \mathrm{i}\chi\nabla^2 A \\ A_t^* &= -(1-\mathrm{i}\theta)A^* - \beta\frac{(1+\mathrm{i}\Delta)}{\mathcal{D}}B^* - \mathrm{i}\chi\nabla^2 A^* \\ \varepsilon_1 B_t &= (1+\mathrm{i}\Delta)(A + C + AC - B) \\ \varepsilon_1 B_t^* &= (1-\mathrm{i}\Delta)(A^* + C + A^*C - B^*)\end{aligned}$$

$$\varepsilon_2(1+\Delta^2)C_t = -(1+\Delta^2)C - \tfrac{1}{2}(1-\mathrm{i}\Delta)\alpha(A^*+B+A^*B) - \tfrac{1}{2}(1+\mathrm{i}\Delta)\alpha(A+B^*+AB^*).$$

We seek a solution of the form

$$[A, A^*, B, B^*, C](x,t) = [k_1, k_2, k_3, k_4, k_5]\mathrm{e}^{\sigma t}\cos(qx).$$

Examine

$$\left[k_j \mathrm{e}^{\sigma t}\cos(qx)\right]_t = \sigma k_j \mathrm{e}^{\sigma t}\cos(qx)$$
$$\nabla^2\left[k_j \mathrm{e}^{\sigma t}\cos(qx)\right] = \left[k_j \mathrm{e}^{\sigma t}\cos(qx)\right]_{xx} = -q^2 k_j \mathrm{e}^{\sigma t}\cos(qx).$$

Thus:

A:

$$\sigma k_1 \mathrm{e}^{\sigma t}\cos(qx) =$$
$$= -(1+\mathrm{i}\theta)k_1 \mathrm{e}^{\sigma t}\cos(qx) - \beta(1-\mathrm{i}\Delta)k_3 \mathrm{e}^{\sigma t}\cos(qx)/\mathcal{D} - \mathrm{i}\chi q^2 k_1 \mathrm{e}^{\sigma t}\cos(qx)$$

or $$\sigma k_1 = -(1+\mathrm{i}\theta)k_1 - \beta(1-\mathrm{i}\Delta)k_3/\mathcal{D} - \mathrm{i}\chi q^2 k_1.$$

A^*:

$$\sigma k_2 \mathrm{e}^{\sigma t}\cos(qx) =$$
$$= -(1-\mathrm{i}\theta)k_2 \mathrm{e}^{\sigma t}\cos(qx) - \beta(1+\mathrm{i}\Delta)k_4 \mathrm{e}^{\sigma t}\cos(qx)/\mathcal{D} + \mathrm{i}\chi q^2 k_2 \mathrm{e}^{\sigma t}\cos(qx)$$

or $$\sigma k_2 = -(1-\mathrm{i}\theta)k_2 - \beta(1+\mathrm{i}\Delta)k_4/\mathcal{D} + \mathrm{i}\chi q^2 k_2.$$

B:

$$\varepsilon_1\sigma k_3 e^{\sigma t}\cos(qx) =$$
$$= (1+\mathrm{i}\Delta)\left(k_1 e^{\sigma t}\cos(qx) + k_5 e^{\sigma t}\cos(qx) + k_1 k_5 e^{2\sigma t}\cos^2(qx) - k_3 e^{\sigma t}\cos(qx)\right)$$

or $\qquad \varepsilon_1\sigma k_3 = (1+\mathrm{i}\Delta)(k_1 - k_3 + k_5) + (1+\mathrm{i}\Delta)k_1 k_5 e^{\sigma t}\cos(qx).$

B^*:

$$\varepsilon_1\sigma k_4 e^{\sigma t}\cos(qx) =$$
$$= (1-\mathrm{i}\Delta)\left(k_2 e^{\sigma t}\cos(qx) + k_5 e^{\sigma t}\cos(qx) + k_2 k_5 e^{2\sigma t}\cos^2(qx) - k_4 e^{\sigma t}\cos(qx)\right)$$

or $\qquad \varepsilon_1\sigma k_4 = (1-\mathrm{i}\Delta)(k_2 - k_4 + k_5) + (1-\mathrm{i}\Delta)k_2 k_5 e^{\sigma t}\cos(qx).$

C:

$$\varepsilon_2(1+\Delta^2)\sigma k_5 e^{\sigma t}\cos(qx) = -(1+\Delta^2)k_5 e^{\sigma t}\cos(qx) +$$
$$-\tfrac{1}{2}(1-\mathrm{i}\Delta)\alpha\left[k_2 e^{\sigma t}\cos(qx) + k_3 e^{\sigma t}\cos(qx) + k_2 k_3 e^{2\sigma t}\cos^2(qx)\right] +$$
$$-\tfrac{1}{2}(1+\mathrm{i}\Delta)\alpha\left[k_1 e^{\sigma t}\cos(qx) + k_4 e^{\sigma t}\cos(qx) + k_1 k_4 e^{2\sigma t}\cos^2(qx)\right]$$

or

$$\varepsilon_2(1+\Delta^2)\sigma k_5 = -(1+\Delta^2)k_5 - \tfrac{1}{2}(1-\mathrm{i}\Delta)\alpha(k_2+k_3) - \tfrac{1}{2}(1+\mathrm{i}\Delta)\alpha(k_1+k_4) +$$
$$-\tfrac{1}{2}(1-\mathrm{i}\Delta)\alpha k_2 k_3 e^{\sigma t}\cos(qx) - \tfrac{1}{2}(1+\mathrm{i}\Delta)\alpha k_1 k_4 e^{\sigma t}\cos(qx).$$

Ignoring terms of $\mathcal{O}(k_p k_r)$, we have an eigenvalue problem of order 5, which has nontrivial solutions when

$$p(\sigma) = \det \begin{bmatrix} \sigma + a & 0 & \beta b^*/\mathcal{D} & 0 & 0 \\ 0 & \sigma + a^* & 0 & \beta b/\mathcal{D} & 0 \\ -b & 0 & \varepsilon_1 \sigma + b & 0 & -b \\ 0 & -b^* & 0 & \varepsilon_1 \sigma + b^* & -b^* \\ \frac{1}{2} b\alpha & \frac{1}{2} b^* \alpha & \frac{1}{2} b^* \alpha & \frac{1}{2} b\alpha & (\varepsilon_2 \sigma + 1)(1 + \Delta^2) \end{bmatrix} = 0,$$

where

$$a = 1 + \mathrm{i}(\theta + \chi q^2),$$
$$b = 1 + \mathrm{i}\Delta,$$

and a star indicates complex conjugation.

Then

$$p(\sigma) = (\sigma + a) \det \begin{bmatrix} \sigma + a^* & 0 & \beta b/\mathcal{D} & 0 \\ 0 & \varepsilon_1 \sigma + b & 0 & -b \\ -b^* & 0 & \varepsilon_1 \sigma + b^* & -b^* \\ \frac{1}{2} b^* \alpha & \frac{1}{2} b^* \alpha & \frac{1}{2} b \alpha & (\varepsilon_2 \sigma + 1)(1 + \Delta^2) \end{bmatrix} +$$

$$+ \frac{\beta b^*}{\mathcal{D}} \det \begin{bmatrix} 0 & \sigma + a^* & \beta b/\mathcal{D} & 0 \\ -b & 0 & 0 & -b \\ 0 & -b^* & \varepsilon_1 \sigma + b^* & -b^* \\ \frac{1}{2} b \alpha & \frac{1}{2} b^* \alpha & \frac{1}{2} b \alpha & (\varepsilon_2 \sigma + 1)(1 + \Delta^2) \end{bmatrix}.$$

Let $\Delta = \Delta_c = 0$, $q^2 = q_c^2 = -\theta/\chi$. Then

$$p(\sigma) = (\sigma + 1) \det \begin{bmatrix} \sigma + 1 & 0 & \beta/\mathcal{D} & 0 \\ 0 & \varepsilon_1 \sigma + 1 & 0 & -1 \\ -1 & 0 & \varepsilon_1 \sigma + 1 & -1 \\ \alpha/2 & \alpha/2 & \alpha/2 & \varepsilon_2 \sigma + 1 \end{bmatrix} +$$

$$+ \frac{\beta}{\mathcal{D}} \det \begin{bmatrix} 0 & \sigma + 1 & \beta/\mathcal{D} & 0 \\ -1 & 0 & 0 & -1 \\ 0 & -1 & \varepsilon_1 \sigma + 1 & -1 \\ \alpha/2 & \alpha/2 & \alpha/2 & \varepsilon_2 \sigma + 1 \end{bmatrix}$$

or

$$p(\sigma) = (\sigma+1)\left\{(\sigma+1)\det\begin{bmatrix}\varepsilon_1\sigma+1 & 0 & -1\\ 0 & \varepsilon_1\sigma+1 & -1\\ \alpha/2 & \alpha/2 & \varepsilon_2\sigma+1\end{bmatrix}+\right.$$

$$\left.+\frac{\beta}{\mathcal{D}}\det\begin{bmatrix}0 & \varepsilon_1\sigma+1 & -1\\ -1 & 0 & -1\\ \alpha/2 & \alpha/2 & \varepsilon_2\sigma+1\end{bmatrix}\right\}+$$

$$+\frac{\beta}{\mathcal{D}}\left\{-(\sigma+1)\det\begin{bmatrix}-1 & 0 & -1\\ 0 & \varepsilon_1\sigma+1 & -1\\ \alpha/2 & \alpha/2 & \varepsilon_2\sigma+1\end{bmatrix}+\right.$$

$$\left.+\frac{\beta}{\mathcal{D}}\det\begin{bmatrix}-1 & 0 & -1\\ 0 & -1 & -1\\ \alpha/2 & \alpha/2 & \varepsilon_2\sigma+1\end{bmatrix}\right\},$$

and thus

$$
\begin{aligned}
p(\sigma) &= (\sigma+1)^2\{(\varepsilon_1\sigma+1)[(\varepsilon_1\sigma+1)(\varepsilon_2\sigma+1)+\alpha/2]+\alpha(\varepsilon_1\sigma+1)/2\}+\\
&\quad+\beta(\sigma+1)\{-(\varepsilon_1\sigma+1)[\alpha/2-(\varepsilon_2\sigma+1)]+\alpha/2\}/\mathcal{D}+\\
&\quad-\beta(\sigma+1)\{-[(\varepsilon_1\sigma+1)(\varepsilon_2\sigma+1)+\alpha/2]+(\varepsilon_1\sigma+1)\alpha/2\}/\mathcal{D}+\\
&\quad+\beta^2\{-[-(\varepsilon_2\sigma+1)+\alpha/2]-\alpha/2\}/\mathcal{D}^2\\
&= (\sigma+1)^2\{(\varepsilon_1\sigma+1)^2(\varepsilon_2\sigma+1)+\alpha(\varepsilon_1\sigma+1)\}+\\
&\quad+\beta(\sigma+1)[2(\varepsilon_1\sigma+1)(\varepsilon_2\sigma+1)-\alpha(\varepsilon_1\sigma+1)+\alpha]/\mathcal{D}+\\
&\quad+\beta^2(\varepsilon_2\sigma+1-\alpha)/\mathcal{D}^2.
\end{aligned}
$$

Assume that $\sigma \sim 1/\varepsilon$, $\sigma+1 \sim \sigma$, $\varepsilon_{1,2} \sim \varepsilon$. Then $\varepsilon\sigma \sim 1$, $\varepsilon^2\sigma \to 0$ as $\varepsilon \to 0$, and multiplying by ε^2,

$$
\begin{aligned}
\varepsilon^2 p(\sigma) &= \varepsilon^2\sigma^2\{(\varepsilon\sigma+1)^2(\varepsilon\sigma+1)+\alpha(\varepsilon\sigma+1)\}+\\
&\quad+\beta\varepsilon^2\sigma\{2(\varepsilon\sigma+1)(\varepsilon\sigma+1)-\alpha\varepsilon\sigma\}/\mathcal{D}+\beta^2\varepsilon^2(\varepsilon\sigma+1-\alpha)/\mathcal{D}^2\\
&\sim \varepsilon^2\sigma^2\left[(\varepsilon\sigma+1)^3+\alpha(\varepsilon\sigma+1)\right] \quad \text{as } \varepsilon \to 0.
\end{aligned}
$$

This implies that

$$
\sigma^2\left[(\varepsilon\sigma+1)^3+\alpha(\varepsilon\sigma+1)\right] = \sigma^2(\varepsilon\sigma+1)[(\varepsilon\sigma+1)^2+\alpha] = 0,
$$

whose roots are

$$
\sigma_{1,2} \sim 0, \quad \sigma_3 \sim -1/\varepsilon, \quad \sigma_{4,5} \sim (-1 \pm i\alpha^{1/2})/\varepsilon.
$$

The roots $\sigma_{1,2}$ correspond to the growth rates σ_R and σ_I, while the remaining roots, $\sigma_{3,4,5}$, have negative real part and therefore they are stabilizing.

D Derivation of the Modified Swift-Hohenberg Equation

$$A_t \sim \sum_{n=1}^{3} \sum_{i=0}^{n} \frac{1}{(n-l)!\, l!} \frac{\partial^n F(0,0)}{\partial A^{n-l} \partial A^{*l}} A^{n-l} A^{*l} + \mathrm{i}\chi \nabla^2 A, \tag{D.1}$$

where

$$F(A, A^*) = -(1+A)\left[1 + \mathrm{i}\theta + \frac{\beta(1-\mathrm{i}\Delta)}{1+\Delta^2+\alpha(1+A)(1+A^*)}\right], \tag{D.2}$$

and

$$A = R + \mathrm{i}I, \quad \mathcal{D} = 1 + \Delta^2 + \alpha.$$

The first derivatives of equation (D.2)

$$\frac{\partial F}{\partial A}(A, A^*) = -1 - \frac{\beta(1+\Delta^2)}{[1+\Delta^2+\alpha(1+A)(1+A^*)]^2} + \\ + \mathrm{i}\left[\frac{\beta\Delta(1+\Delta^2)}{[1+\Delta^2+\alpha(1+A)(1+A^*)]^2} - \theta\right]$$

$$\frac{\partial F}{\partial A^*}(A, A^*) = \frac{\beta\alpha(1-\mathrm{i}\Delta)(1+A)^2}{[1+\Delta^2+\alpha(1+A)(1+A^*)]^2}$$

$$\frac{\partial F}{\partial A}(0,0) = -1 - \frac{\beta(1+\Delta^2)}{\mathcal{D}^2} + \mathrm{i}\left[\frac{\beta\Delta(1+\Delta^2)}{\mathcal{D}^2} - \theta\right]$$

$$\frac{\partial F}{\partial A^*}(0,0) = \frac{\beta\alpha(1-\mathrm{i}\Delta)}{\mathcal{D}^2}.$$

The second derivatives of equation (D.2)

$$\frac{\partial^2 F}{\partial A^2}(A, A^*) = \frac{2\beta\alpha(1+\Delta^2)(1-\mathrm{i}\Delta)(1+A^*)}{[1+\Delta^2+\alpha(1+A)(1+A^*)]^3}$$

$$\frac{1}{2}\frac{\partial^2 F}{\partial A^2}(0,0) = \frac{\beta\alpha(1+\Delta^2)(1-\mathrm{i}\Delta)}{\mathcal{D}^3}$$

$$\frac{\partial^2 F}{\partial A^{*2}}(A, A^*) = \frac{-2\beta\alpha^2(1-\mathrm{i}\Delta)(1+A^*)^3}{[1+\Delta^2+\alpha(1+A)(1+A^*)]^3}$$

$$\frac{1}{2}\frac{\partial^2 F}{\partial A^{*2}}(0,0) = \frac{-\beta\alpha^2(1-\mathrm{i}\Delta)}{\mathcal{D}^3}$$

$$\frac{\partial^2 F}{\partial A\,\partial A^*}(A, A^*) = \frac{2\beta\alpha(1+\Delta^2)(1-\mathrm{i}\Delta)(1+A)}{[1+\Delta^2+\alpha(1+A)(1+A^*)]^3}$$

$$\frac{\partial^2 F}{\partial A^2}(0,0) = \frac{2\beta\alpha(1+\Delta^2)(1-\mathrm{i}\Delta)}{\mathcal{D}^3}.$$

The third derivatives of equation (D.2)

$$\frac{\partial^3 F}{\partial A^3}(A, A^*) = \frac{-6\beta\alpha^2(1+\Delta^2)(1-\mathrm{i}\Delta)(1+A^*)^2}{[1+\Delta^2+\alpha(1+A)(1+A^*)]^4}$$

$$\frac{1}{3!}\frac{\partial^3 F}{\partial A^3}(0,0) = \frac{-\beta\alpha^2(1+\Delta^2)(1-\mathrm{i}\Delta)}{\mathcal{D}^4}$$

$$\frac{\partial^3 F}{\partial A^2\,\partial A^*}(A, A^*) = \frac{2\beta\alpha(1+\Delta^2)(1-\mathrm{i}\Delta)[1+\Delta^2-2\alpha(1+A)(1+A^*)]}{[1+\Delta^2+\alpha(1+A)(1+A^*)]^4}$$

$$\frac{1}{2}\frac{\partial^3 F}{\partial A^2\,\partial A^*}(0,0) = \frac{\beta\alpha(1+\Delta^2)(1-\mathrm{i}\Delta)(1+\Delta^2-2\alpha)}{\mathcal{D}^4}$$

$$\frac{\partial^3 F}{\partial A\,\partial A^{*2}}(A, A^*) = \frac{-6\beta\alpha^2(1+\Delta^2)(1-\mathrm{i}\Delta)(1+A)^2}{[1+\Delta^2+\alpha(1+A)(1+A^*)]^4}$$

$$\frac{1}{2}\frac{\partial^3 F}{\partial A\,\partial A^{*2}}(0,0) = \frac{-3\beta\alpha^2(1+\Delta^2)(1-\mathrm{i}\Delta)}{\mathcal{D}^4}$$

$$\frac{\partial^3 F}{\partial A^{*3}}(A, A^*) = \frac{6\beta\alpha^3(1-\mathrm{i}\Delta)(1+A)^4}{[1+\Delta^2+\alpha(1+A)(1+A^*)]^4}$$

$$\frac{1}{3!}\frac{\partial^3 F}{\partial A^{*3}}(0,0) = \frac{\beta\alpha^3(1-\mathrm{i}\Delta)}{\mathcal{D}^4}.$$

Let $\Delta = 0$ and $A = R + \mathrm{i}I$. Then equation (D.1) becomes

$$
\begin{aligned}
R_t + \mathrm{i}I_t = &\left[-1 - \frac{\beta}{(1+\alpha)^2} - \mathrm{i}\theta\right](R + \mathrm{i}I) + \\
&+ \left[\frac{\beta\alpha}{(1+\alpha)^2}\right](R - \mathrm{i}I) + \\
&+ \left[\frac{\beta\alpha}{(1+\alpha)^3}\right](R^2 + 2\mathrm{i}RI - I^2) + \\
&+ \left[\frac{2\beta\alpha}{(1+\alpha)^3}\right](R^2 + I^2) + \\
&+ \left[\frac{-\beta\alpha^2}{(1+\alpha)^3}\right](R^2 + 2\mathrm{i}RI - I^2) + \\
&+ \mathrm{i}\chi\left[\nabla^2 R + \mathrm{i}\nabla^2 I\right] + \\
&+ \left[\frac{-\beta\alpha^2}{(1+\alpha)^4}\right](R^3 + 3\mathrm{i}R^2 I - 3RI^2 - \mathrm{i}I^3) + \\
&+ \left[\frac{\beta\alpha(1-2\alpha)}{(1+\alpha)^4}\right](R^3 + \mathrm{i}R^2 I + RI^2 + \mathrm{i}I^3) + \\
&+ \left[\frac{-3\beta\alpha^2}{(1+\alpha)^4}\right](R^3 - \mathrm{i}R^2 I + RI^2 - \mathrm{i}I^3) + \\
&+ \left[\frac{\beta\alpha^3}{(1+\alpha)^4}\right](R^3 - 3\mathrm{i}R^2 I - 3RI^2 + \mathrm{i}I^3).
\end{aligned}
\tag{D.3}
$$

Examining the real coefficients of equation (D.3), we have

$\mathcal{O}(R)$**:**

$$-1 + \frac{-\beta + \beta\alpha}{(1+\alpha)^2} = -1 + \frac{\beta(\alpha - 1)}{(1+\alpha)^2} = \sigma_R(\alpha, \beta).$$

$\mathcal{O}(I)$**:**

$$\theta = -\chi q_c^2.$$

Spatial:

$$-\chi \nabla^2 I.$$

$\mathcal{O}(R^2)$**:**

$$\frac{\beta\alpha + 2\beta\alpha - \beta\alpha^2}{(1+\alpha)^3} = \frac{\beta\alpha(3-\alpha)}{(1+\alpha)^3} = -\omega_0(\alpha, \beta).$$

$\mathcal{O}(I^2)$**:**

$$\frac{-\beta\alpha + 2\beta\alpha + \beta\alpha^2}{(1+\alpha)^3} = \frac{\beta\alpha}{(1+\alpha)^2}.$$

$\mathcal{O}(R^3)$**:**

$$\frac{-\beta\alpha^2 + \beta\alpha(1-2\alpha) - 3\beta\alpha^2 + \beta\alpha^3}{(1+\alpha)^4} = \frac{\beta\alpha\Big[(\alpha-3)^2 - 8\Big]}{(1+\alpha)^4} = -\omega_1(\alpha, \beta).$$

$\mathcal{O}(RI^2)$**:**

$$\frac{3\beta\alpha^2 + \beta\alpha(1-2\alpha) - 3\beta\alpha^2 - 3\beta\alpha^3}{(1+\alpha)^4} = \frac{\beta\alpha(1-3\alpha)}{(1+\alpha)^3}.$$

Examining the imaginary coefficients of equation (D.3), we have

$\mathcal{O}(R)$**:**

$$-\theta = \chi q_c^2.$$

Spatial:

$$-\chi \nabla^2 R.$$

$\mathcal{O}(I)$**:**

$$-1 - \frac{\beta + \beta\alpha}{(1+\alpha)^2} = -\left(1 + \frac{\beta}{1+\alpha}\right) = \sigma_I(\alpha, \beta).$$

$\mathcal{O}(RI)$**:**

$$\frac{2\beta\alpha - 2\beta\alpha^2}{(1+\alpha)^3} = \frac{2\beta\alpha(1-\alpha)}{(1+\alpha)^3}.$$

$\mathcal{O}(R^2 I)$**:**

$$\frac{-3\beta\alpha^2 + \beta\alpha(1-2\alpha) + 3\beta\alpha^2 - 3\beta\alpha^3}{(1+\alpha)^4} = \frac{\beta\alpha(1-3\alpha)}{(1+\alpha)^3}.$$

$\mathcal{O}(I^3)$**:**

$$\frac{\beta\alpha^2 + \beta\alpha(1-2\alpha) + 3\beta\alpha^2 + \beta\alpha^3}{(1+\alpha)^4} = \frac{\beta\alpha}{(1+\alpha)^2}.$$

Then

$$
\begin{aligned}
R_t = &\left[-1 + \frac{\beta(\alpha-1)}{(1+\alpha)^2}\right] R + \\
&+ \frac{\beta\alpha(3-\alpha)}{(1+\alpha)^3} R^2 + \\
&+ \frac{\beta\alpha\left[(\alpha+1)^2 - 8\alpha\right]}{(1+\alpha)^4} R^3 + \\
&- \chi(\nabla^2 + q_c^2) I + \\
&+ \frac{\beta\alpha}{(1+\alpha)^2} I^2 + \\
&+ \frac{\beta\alpha(1-3\alpha)}{(1+\alpha)^3} R I^2,
\end{aligned}
\tag{D.4}
$$

and

$$
\begin{aligned}
I_t = &\chi(\nabla^2 + q_c^2) R + \\
&+ \sigma_I(\alpha, \beta) I \\
&+ \frac{2\beta\alpha(1-\alpha)}{(1+\alpha)^3} I R + \\
&+ \frac{\beta\alpha(1-3\alpha)}{(1+\alpha)^3} I R^2 + \\
&+ \frac{\beta\alpha}{(1+\alpha)^2} I^3,
\end{aligned}
\tag{D.5}
$$

where

$$
I \sim -\left[\chi/\sigma_I(\alpha, \beta)\right]\left(\nabla^2 + q_c^2\right) R. \tag{D.6}
$$

Upon substituting equation (D.6) into equation (D.4), we obtain

$$R_t \sim \sigma_R(\alpha,\beta)R - \omega_0(\alpha,\beta)R^2 - \omega_1(\alpha,\beta)R^3 + \left[\frac{\chi^2}{\sigma_I(\alpha,\beta)}\right]\left(\nabla^2 + q_c^2\right)^2 R,$$

where

$$\begin{aligned}
\sigma_R(\alpha,\beta) &= -1 + \frac{\beta(\alpha-1)}{(\alpha+1)^2} \\
\sigma_I(\alpha,\beta) &= -1 - \frac{\beta}{\alpha+1} \\
\chi q_c^2 &= -\theta = 1 \\
\omega_0(\alpha,\beta) &= \frac{\beta\alpha(\alpha-3)}{(\alpha+1)^3} \\
\omega_1(\alpha,\beta) &= \frac{\beta\alpha[8\alpha-(\alpha+1)^2]}{(\alpha+1)^4}.
\end{aligned}$$

E One-Dimensional Analysis

According to [15], we seek a solution to (2.9) of the form

$$R(x,y,t) \sim A_1(t)\cos(q_c x) + A_1^2(t)[R_{20} + R_{22}\cos(2q_c x)] + \\ + A_1^3(t)[R_{31}\cos(q_c x) + R_{33}\cos(3q_c x)],$$

where

$$\dot{A}_1(t) \sim \sigma A_1(t) - a_1 A_1^3(t).$$

Calculation of each term in Eq. (2.9)

$$\begin{aligned} R_t &\sim \dot{A}_1\cos(q_c x) + 2A_1\dot{A}_1[R_{20} + R_{22}\cos(2q_c x)] + \\ &\quad + 3A_1^2\dot{A}_1[R_{31}\cos(q_c x) + R_{33}\cos(3q_c x)] \\ &\sim \sigma(A_1 - a_1 A_1^3)\cos(q_c x) + 2\sigma A_1^2[R_{20} + R_{22}\cos(2q_c x)] + \\ &\quad + 3\sigma A_1^3[R_{31}\cos(q_c x) + R_{33}\cos(3q_c x)] \\ &= \sigma A_1\cos(q_c x) + 2\sigma A_1^2[R_{20} + R_{22}\cos(2q_c x)] + \\ &\quad + A_1^3[(3\sigma R_{31} - a_1)\cos(q_c x) + 3\sigma R_{33}\cos(3q_c x)]. \end{aligned}$$

$$
\begin{aligned}
R^2 &\sim A_1^2 \cos^2(q_c x) + 2A_1^3[R_{20}\cos(q_c x) + R_{22}\cos(2q_c x)] \\
&= \tfrac{1}{2}A_1^2[1 + \cos(2q_c x)] + \\
&\quad + A_1^3[2R_{20}\cos(q_c x) + R_{22}\{\cos(q_c x) + \cos(3q_c x)\}] \\
&= \tfrac{1}{2}A_1^2[1 + \cos(2q_c x)] + \\
&\quad + A_1^3[(2R_{20} + R_{22})\cos(q_c x) + R_{22}\cos(3q_c x)].
\end{aligned}
$$

$$
R^3 \sim A_1^3 \cos^3(q_c x) = \tfrac{1}{4}A_1^3[3\cos(q_c x) + \cos(3q_c x)].
$$

$$
\begin{aligned}
\left(\nabla^2 + q_c^2\right)^2 R &\sim A_1^2[q_c^4 R_{20} + R_{22}(-4q_c^2 + q_c^2)^2\cos(2q_c x)] + \\
&\quad + A_1^3 R_{33}(-9q_c^2 + q_c^2)^2\cos(3q_c x) \\
&= q_c^4\left[A_1^2[R_{20} + 9R_{22}\cos(2q_c x)] + 64A_1^3 R_{33}\cos(3q_c x)\right].
\end{aligned}
$$

Determining the coefficients of R

$\mathcal{O}\left(A_1 \cos(q_c x)\right)$:

$$\sigma = \sigma_R.$$

$\mathcal{O}\left(A_1^2\right)$:

$$2\sigma R_{20} = \sigma_R R_{20} + \left(\frac{\chi^2}{\sigma_I}\right) q_c^4 R_{20} - \frac{\omega_0}{2}$$

or

$$R_{20} = \frac{\omega_2/2}{\sigma_I^{-1} - \sigma_R}.$$

$\mathcal{O}\left(A_1^2 \cos(2q_c x)\right)$:

$$2R_{22} = \sigma_R R_{22} + 9\left(\frac{\chi^2}{\sigma_I}\right) q_c^4 R_{20} - \frac{\omega_0}{2}$$

or

$$R_{22} = \frac{\omega_2/2}{9\sigma_I^{-1} - \sigma_R}.$$

$\mathcal{O}\left(A_1^3 \cos(3q_c x)\right)$:

$$3\sigma R_{31} - a_1 = \sigma_R R_{31} - \omega_0(2R_{20} + R_{22}) - \frac{3\omega_1}{4}.$$

Applying the Fredholm solvability condition to this last equation (*i.e.*, taking the limit as $\beta \to \beta_0$), we get

$$a_1 = \left[\omega_0(2R_{20} + R_{22}) + \frac{3\omega_1}{4}\right]_{\beta=\beta_0}$$

where

$$\beta_0(\alpha) = \frac{(\alpha+1)^2}{\alpha-1}.$$

for $\alpha > 1$.

Now,

$$\begin{aligned}
\sigma_R[\alpha, \beta_0(\alpha)] &= 0, \\
\sigma_I[\alpha, \beta_0(\alpha)] &= -1 - \frac{\beta_0(\alpha)}{\alpha+1} = -1 - \frac{\alpha+1}{\alpha-1} = \frac{-2\alpha}{\alpha-1}, \\
R_{20}[\alpha, \beta_0(\alpha)] &= \tfrac{1}{2}\omega_0\sigma_I[\alpha, \beta_0(\alpha)],
\end{aligned}$$

and

$$R_{22}[\alpha, \beta_0(\alpha)] = \tfrac{1}{18}\omega_0\sigma_I[\alpha, \beta_0(\alpha)],$$

so

$$\begin{aligned}
a_1 &= \tfrac{19}{18}\omega_1^2\sigma_I + \tfrac{3}{4}\omega_1 \\
&= \frac{-19\beta_0^2\alpha^3(\alpha-3)^2}{9(\alpha+1)^6(\alpha-1)} + \frac{3\beta_0\alpha[8\alpha-(\alpha+1)^2]}{4(\alpha+1)^4} \\
&= \frac{\alpha\beta_0}{(\alpha+1)^4}\left\{-\frac{19}{9}\left[\frac{\alpha(\alpha-3)}{\alpha-1}\right]^2 + \frac{3}{4}[8\alpha-(\alpha+1)^2]\right\}.
\end{aligned}$$

F Two-Dimensional Analysis

According to [15], we seek a solution to (2.9) of the form

$$\begin{aligned} R(x,y,t) \sim\ & A_1(t)\cos(q_c x) + B_1(t)\cos(q_c z) + A_1^2(t)R_{20}(x) + \\ & + A_1(t)B_1(t)R_{11}(x,z) + B_1^2(t)R_{02}(z) + A_1^3(t)R_{30}(x) + A_1^2(t)B_1(t)R_{21}(x,z) + \\ & + A_1(t)B_1^2(t)R_{12}(x,z) + B_1^3(t)R_{03}(z), \end{aligned} \tag{F.1}$$

where

$$\begin{aligned} z &= x\cos(\psi) + y\sin(\psi) \\ R_{20}(x) &= R_{2000} + R_{2020}\cos(2q_c x) \\ R_{11}(x,z) &= R_{1111}\cos[q_c(x+z)] + R_{111(-1)}\cos[q_c(x-z)] \\ R_{02}(x) &= R_{0200} + R_{0202}\cos(2q_c z) \\ R_{30}(x) &= R_{3010}\cos(q_c x) + R_{3030}\cos(3q_c x) \\ R_{21}(x,z) &= R_{2101}\cos(q_c z) + R_{2121}\cos[q_c(2x+z)] + R_{212(-1)}\cos[q_c(2x-z)] \\ R_{12}(x,z) &= R_{1210}\cos(q_c x) + R_{1212}\cos[q_c(x+2z)] + R_{121(-2)}\cos[q_c(x-2z)] \\ R_{03}(x) &= R_{0301}\cos(q_c z) + R_{0303}\cos(3q_c z), \end{aligned}$$

and A_1, B_1 satisfy the Landau Equations

$$\frac{\mathrm{d}A_1}{\mathrm{d}t} \sim \sigma A_1 - A_1(a_1 A_1^2 + b_1 B_1^2) \tag{F.2a}$$

$$\frac{\mathrm{d}B_1}{\mathrm{d}t} \sim \sigma B_1 - B_1(b_1 A_1^2 + a_1 B_1^2). \tag{F.2b}$$

Calculation of each term in Eq. (2.9)

R and its time derivative

$$
\begin{aligned}
R \sim\ & A_1 \cos(q_c x) + B_1 \cos(q_c z) + A_1^2 R_{20}(x) + A_1 B_1 R_{11}(x,z) + B_1^2 R_{02}(z) + \\
& + A_1^3 [R_{3010} \cos(q_c x) + R_{3030} \cos(3 q_c x)] + \\
& + A_1^2 B_1 \{R_{2101} \cos(q_c z) + R_{2121} \cos[q_c(2x+z)] + R_{212(-1)} \cos[q_c(2x-z)]\} + \\
& + A_1 B_1^2 \{R_{1210} \cos(q_c x) + R_{1212} \cos[q_c(x+2z)] + R_{121(-2)} \cos[q_c(x-2z)]\} + \\
& + B_1^3 [R_{0301} \cos(q_c z) + R_{0303} \cos(3 q_c z)].
\end{aligned}
$$

$$
\begin{aligned}
R_t \sim\ & \dot{A}_1 \cos(q_c x) + \dot{B}_1 \cos(q_c z) + 2A_1\dot{A}_1 R_{20}(x) + (\dot{A}_1 B_1 + A_1 \dot{B}_1) R_{11}(x,z) + \\
& + 2B_1\dot{B}_1 R_{02}(z) + 3A_1^2\dot{A}_1 R_{30}(x) + (2A_1\dot{A}_1 B_1 + A_1^2\dot{B}_1) R_{21}(x,z) + \\
& + (\dot{A}_1 B_1^2 + 2A_1 B_1 \dot{B}_1) R_{12}(x,z) + 3B_1^2\dot{B}_1 R_{03}(z) \\
= & \left[\sigma A_1 - A_1(a_1 A_1^2 + b_1 B_1^2)\right] \cos(q_c x) + \left[\sigma B_1 - B_1(b_1 A_1^2 + a_1 B_1^2)\right] \cos(q_c z) + \\
& + 2A_1\left[\sigma A_1 - A_1(a_1 A_1^2 + b_1 B_1^2)\right] R_{20}(x) + \\
& + \Big\{\left[\sigma A_1 - A_1(a_1 A_1^2 + b_1 B_1^2)\right] B_1 + A_1\left[\sigma B_1 - B_1(b_1 A_1^2 + a_1 B_1^2)\right]\Big\} R_{11}(x,z) + \\
& + 2B_1\left[\sigma B_1 - B_1(b_1 A_1^2 + a_1 B_1^2)\right] R_{02}(z) + 3A_1^2\left[\sigma A_1 - A_1(a_1 A_1^2 + b_1 B_1^2)\right] R_{30}(x) + \\
& + \Big\{2A_1 B_1\left[\sigma A_1 - A_1(a_1 A_1^2 + b_1 B_1^2)\right] + A_1^2\left[\sigma B_1 - B_1(b_1 A_1^2 + a_1 B_1^2)\right]\Big\} R_{21}(x,z) + \\
& + \Big\{\left[\sigma A_1 - A_1(a_1 A_1^2 + b_1 B_1^2)\right] B_1^2 + 2A_1 B_1\left[\sigma B_1 - B_1(b_1 A_1^2 + a_1 B_1^2)\right]\Big\} R_{12}(x,z) + \\
& + 3B_1^2\left[\sigma B_1 - B_1(b_1 A_1^2 + a_1 B_1^2)\right] R_{03}(z) \\
= & \sigma A_1 \cos(q_c x) + \sigma B_1 \cos(q_c z) + 2\sigma A_1^2 R_{20}(x) + 2\sigma A_1 B_1 R_{11}(x,z) + 2\sigma B_1^2 R_{02}(z) + \\
& + A_1^3\left[-a_1 \cos(q_c x) + 3\sigma R_{30}(x)\right] + A_1^2 B_1\left[-b_1 \cos(q_c z) + 3\sigma R_{21}(x,z)\right] + \\
& + A_1 B_1^2\left[-b_1 \cos(q_c x) + 3\sigma R_{12}(x,z)\right] + B_1^3\left[-a_1 \cos(q_c z) + 3\sigma R_{03}(z)\right] \\
= & \sigma A_1 \cos(q_c x) + \sigma B_1 \cos(q_c z) + 2\sigma A_1^2 R_{20}(x) + 2\sigma A_1 B_1 R_{11}(x,z) + 2\sigma B_1^2 R_{02}(z) + \\
& + A_1^3\left[(3\sigma R_{3010} - a_1)\cos(q_c x) + 3\sigma R_{3030} \cos(3q_c x)\right] + \\
& + A_1^2 B_1\Big\{(3\sigma R_{2101} - b_1)\cos(q_c z) + 3\sigma R_{2121} \cos[q_c(2x+z)] + \\
& \qquad + 3\sigma R_{212(-1)} \cos[q_c(2x-z)]\Big\} + \\
& + A_1 B_1^2\Big\{(3\sigma R_{1210} - b_1)\cos(q_c x) + 3\sigma R_{1212} \cos[q_c(x+2z)] + \\
& \qquad + 3\sigma R_{121(-2)} \cos[q_c(x-2z)]\Big\} + \\
& + B_1^3\left[(3\sigma R_{0301} - a_1)\cos(q_c z) + 3\sigma R_{0303} \cos(3q_c z)\right].
\end{aligned}
$$

Powers of R

$$
\begin{aligned}
R^2 \sim\ & A_1^2\cos^2(q_c x) + 2A_1B_1\cos(q_c x)\cos(q_c z) + B_1^2\cos^2(q_c z) + \\
& + 2A_1^3 R_{20}\cos(q_c x) + 2A_1^2 B_1[R_{20}(x)\cos(q_c z) + R_{11}(x,z)\cos(q_c x)] + \\
& + 2A_1B_1^2[R_{02}(z)\cos(q_c x) + R_{11}(x,z)\cos(q_c z)] + 2B_1^3 R_{02}\cos(q_c z) \\
=\ & A_1^2[1+\cos(2q_c x)]/2 + A_1B_1\{\cos[q_c(x+z)] + \cos[q_c(x-z)]\} + \\
& + B_1^2[1+\cos(2q_c z)]/2 + 2A_1^3[R_{2000} + R_{2020}\cos(2q_c x)]\cos(q_c x) + \\
& + 2A_1^2B_1\Big\{[R_{2000} + R_{2020}\cos(2q_c x)]\cos(q_c z) + \\
& \qquad + \Big[R_{1111}\cos[q_c(x+z)] + R_{111(-1)}\cos[q_c(x-z)]\Big]\cos(q_c x)\Big\} + \\
& + 2A_1B_1^2\Big\{[R_{0200} + R_{0202}\cos(2q_c z)]\cos(q_c x) + \\
& \qquad + \Big[R_{1111}\cos[q_c(x+z)] + R_{111(-1)}\cos[q_c(x-z)]\Big]\cos(q_c z)\Big\} + \\
& + 2B_1^3[R_{0200} + R_{0202}\cos(2q_c z)]\cos(q_c z) \\
\sim\ & A_1^2[1+\cos(2q_c x)]/2 + A_1B_1\{\cos[q_c(x+z)] + \cos[q_c(x-z)]\} + \\
& + B_1^2[1+\cos(2q_c z)]/2 + A_1^3\left[(2R_{2000} + R_{2020})\cos(q_c x) + R_{2020}\cos(3q_c x)\right] + \\
& + A_1^2B_1\Big\{(2R_{2000} + R_{1111} + R_{111(-1)})\cos(q_c z) + (R_{2020} + R_{1111})\cos[q_c(2x+z)] + \\
& \qquad + (R_{2020} + R_{111(-1)})\cos[q_c(2x-z)]\Big\} + \\
& + A_1B_1^2\Big\{(2R_{0200} + R_{1111} + R_{111(-1)})\cos(q_c x) + (R_{0202} + R_{1111})\cos[q_c(x+2z)] + \\
& \qquad + (R_{0202} + R_{111(-1)})\cos[q_c(x-2z)]\Big\} + \\
& + B_1^3\left[(2R_{0200} + R_{0202}\cos(q_c z) + R_{0202}\cos(3q_c z)\right].
\end{aligned}
$$

$$
\begin{aligned}
R^3 \sim\ & A_1^3\cos^3(q_c x) + 3A_1^2 B_1\cos^2(q_c x)\cos(q_c z) + 3A_1 B_1^2\cos(q_c x)\cos^2(q_c z) + \\
& + B_1^3\cos^3(q_c z) \\
=\ & \tfrac{1}{4}A_1^3\left[\cos(3q_c x) + 3\cos(q_c x)\right] + \tfrac{3}{2}A_1^2 B_1\left[1+\cos(2q_c x)\right]\cos(q_c z) + \\
& + \tfrac{3}{2}A_1 B_1^2\cos(q_c x)\left[1+\cos(2q_c z)\right] + \tfrac{1}{4}B_1^3\left[\cos(3q_c z) + 3\cos(q_c z)\right] \\
=\ & \tfrac{1}{4}A_1^3\left[\cos(3q_c x) + 3\cos(q_c x)\right] + \\
& + \tfrac{3}{4}A_1^2 B_1\left\{2\cos(q_c z) + \cos[q_c(2x+z)] + \cos[q_c(2x-z)]\right\} + \\
& + \tfrac{3}{4}A_1 B_1^2\left\{2\cos(q_c x) + \cos[q_c(x+2z)] + \cos[q_c(x-2z)]\right\} + \\
& + \tfrac{1}{4}B_1^3\left[\cos(3q_c z) + 3\cos(q_c z)\right].
\end{aligned}
$$

Spatial derivatives

We have that

$$
\cos(mx+nz) = \cos[(m+n\cos(\psi))x + ny\sin(\psi)].
$$

Then

$$
\begin{aligned}
\nabla^2\cos(mx+nz) &= -[(m+n\cos(\psi))^2 + (n\sin(\psi))^2]\cos(mx+nz) \\
&= -[m^2 + 2mn\cos(\psi) + n^2]\cos(mx+nz), \\
\nabla^4\cos(mx+nz) &= [m^2 + 2mn\cos(\psi) + n^2]^2\cos(mx+nz).
\end{aligned}
$$

$$\nabla^2 R \sim -q_c^2\Big\{A_1\cos(q_c x) + B_1\cos(q_c z) + 4A_1^2 R_{2020}\cos(2q_c x) +$$
$$+ 2A_1B_1\Big\{R_{1111}[1+\cos(\psi)]\cos[q_c(x+z)] +$$
$$+ R_{111(-1)}[1-\cos(\psi)]\cos[q_c(x-z)]\Big\} +$$
$$+ 4B_1^2 R_{0202}\cos(2q_c z) + A_1^3[R_{3010}\cos(q_c x) + 9R_{3030}\cos(3q_c x)] +$$
$$+ A_1^2B_1\Big\{R_{2101}\cos(q_c z) + R_{2121}[5+4\cos(\psi)]\cos[q_c(2x+z)] +$$
$$+ R_{212(-1)}[5-4\cos(\psi)]\cos[q_c(2x-z)]\Big\} +$$
$$+ A_1B_1^2\Big\{R_{1210}\cos(q_c x) + R_{1212}[5+4\cos(\psi)]\cos[q_c(x+2z)] +$$
$$+ R_{121(-2)}[5-4\cos(\psi)]\cos[q_c(x-2z)]\Big\} +$$
$$+ B_1^3[R_{0301}\cos(q_c z) + 9R_{0303}\cos(3q_c z)]\Big\}.$$

$$\nabla^4 R \sim q_c^4\Big\{A_1\cos(q_c x) + B_1\cos(q_c z) + 16A_1^2 q_c^4 R_{2020}\cos(2q_c x) +$$
$$+ 4A_1B_1\Big\{R_{1111}[1+\cos(\psi)]^2\cos[q_c(x+z)] +$$
$$+R_{111(-1)}[1-\cos(\psi)]^2\cos[q_c(x-z)]\Big\} +$$
$$+ 16B_1^2 R_{0202}\cos(2q_c z) + A_1^3[R_{3010}\cos(q_c x) + 81R_{3030}\cos(3q_c x)] +$$
$$+ A_1^2B_1\Big\{R_{2101}\cos(q_c z) + R_{2121}[5+4\cos(\psi)]^2\cos[q_c(2x+z)] +$$
$$+ R_{212(-1)}[5-4\cos(\psi)]^2\cos[q_c(2x-z)]\Big\} +$$
$$+ A_1B_1^2\Big\{R_{1210}\cos(q_c x) + R_{1212}[5+4\cos(\psi)]^2\cos[q_c(x+2z)] +$$
$$+ R_{121(-2)}[5-4\cos(\psi)]^2\cos[q_c(x-2z)]\Big\} +$$
$$+ B_1^3[R_{0301}\cos(q_c z) + 81R_{0303}\cos(3q_c z)]\Big\}.$$

$$
\begin{aligned}
\left(\nabla^2 + q_c^2\right)^2 R &= \left(\nabla^4 + 2q_c^2\nabla^2 + q_c^4\right) R \\
&\sim q_c^4 \Big\{ A_1^2 \left[R_{2000} + 9R_{2020}\cos(2q_c x) \right] + \\
&\quad + A_1 B_1 \Big\{ R_{1111}[1 + 2\cos(\psi)]^2 \cos[q_c(x+z)] + \\
&\qquad + R_{111(-1)}[1 - 2\cos(\psi)]^2 \cos[q_c(x-z)] \Big\} + \\
&\quad + B_1^2 \left[R_{0200} + 9R_{0202}\cos(2q_c z) \right] + 64 A_1^3 R_{3030}\cos(3q_c x) + \\
&\quad + A_1^2 B_1 \Big\{ R_{2121}[6 + 4\cos(\psi)]^2 \cos[q_c(2x+z)] + \\
&\qquad + R_{212(-1)}[6 - 4\cos(\psi)]^2 \cos[q_c(2x-z)] \Big\} + \\
&\quad + A_1 B_1^2 \Big\{ R_{1212}[6 + 4\cos(\psi)]^2 \cos[q_c(x+2z)] + \\
&\qquad + R_{121(-2)}[6 - 4\cos(\psi)]^2 \cos[q_c(x-2z)] \Big\} + \\
&\quad + 64 B_1^3 R_{0303}\cos(3q_c z) \Big\}.
\end{aligned}
$$

Determining the coefficients of R

$\mathcal{O}(A_1)$:

$\cos(q_c x)$:

$$\sigma = \sigma_R = -1 + \frac{\beta(\alpha - 1)}{(\alpha + 1)^2}.$$

$\mathcal{O}(B_1)$:

$\cos(q_c x)$:

$$\sigma = \sigma_R.$$

Nothing new here.

$\mathcal{O}\left(A_1^2\right)$:

1:

$$2\sigma R_{2000} = \sigma_R R_{2000} - \tfrac{1}{2}\omega_0 + \sigma_I^{-1}\chi^2 q_c^4 R_{2000}$$
$$\left(\sigma_R - \sigma_I^{-1}\right) R_{2000} = -\tfrac{1}{2}\omega_0$$

or

$$R_{2000} = -\frac{\omega_0/2}{\sigma_R - \sigma_I^{-1}}.$$

$\cos(2q_c x)$:

$$2\sigma R_{2020} = \sigma_R R_{2020} - \tfrac{1}{2}\omega_0 + 9\sigma_I^{-1}\chi^2 q_c^4 R_{2020}$$
$$\left(\sigma_R - 9\sigma_I^{-1}\right) R_{2020} = -\tfrac{1}{2}\omega_0$$

or

$$R_{2020} = -\frac{\omega_0/2}{\sigma_R - 9\sigma_I^{-1}}.$$

$\mathcal{O}(A_1 B_1)$:

$\cos[q_c(x+z)]$:

$$2\sigma_R R_{1111} = \sigma_R R_{1111} - \omega_0 + \sigma_I^{-1}\chi^2 q_c^4 [1+2\cos(\psi)]^2 R_{1111}$$
$$\left(\sigma_R - \sigma_I^{-1}[1+2\cos(\psi)]^2\right) R_{1111} = -\omega_0$$

or

$$R_{1111} = -\frac{\omega_0}{\sigma_R - \sigma_I^{-1}[1+2\cos(\psi)]^2}.$$

$\cos[q_c(x-z)]$:

$$2\sigma_R R_{111(-1)} = \sigma_R R_{111(-1)} - \omega_0 + \sigma_I^{-1}\chi^2 q_c^4 [1-2\cos(\psi)]^2 R_{111(-1)}$$
$$\left(\sigma_R - \sigma_I^{-1}[1-2\cos(\psi)]^2\right) R_{111(-1)} = -\omega_0$$

or

$$R_{111(-1)} = -\frac{\omega_0}{\sigma_R - \sigma_I^{-1}[1-2\cos(\psi)]^2}.$$

$\mathcal{O}\left(B_1^2\right)$:

1:

$$2\sigma R_{0200} = \sigma_R R_{0200} - \tfrac{1}{2}\omega_0 + \sigma_I^{-1}\chi^2 q_c^4 R_{0200}$$
$$\left(\sigma_R - \sigma_I^{-1}\right) R_{0200} = -\tfrac{1}{2}\omega_0$$

or

$$R_{0200} = -\frac{\omega_0/2}{\sigma_R - \sigma_I^{-1}} = R_{2000}.$$

$\cos(2q_c z)$:

$$2\sigma R_{0202} = \sigma_R R_{0202} - \tfrac{1}{2}\omega_0 + 9\sigma_I^{-1}\chi^2 q_c^4 R_{0202}$$
$$\left(\sigma_R - 9\sigma_I^{-1}\right) R_{0202} = -\tfrac{1}{2}\omega_0$$

or

$$R_{0202} = -\frac{\omega_0/2}{\sigma_R - 9\sigma_I^{-1}} = R_{2020}.$$

$\mathcal{O}\left(A_1^3\right)$:

$\cos(q_c x)$:

$$3\sigma R_{3010} - a_1 = \sigma_R R_{3010} - (2R_{2000} + R_{2020})\omega_0 - \tfrac{3}{4}\omega_1$$

$$2\sigma_R R_{3010} = a_1 - (2R_{2000} + R_{2020})\omega_0 - \tfrac{3}{4}\omega_1$$

or

$$R_{3010} = \frac{a_1 - (2R_{2000} + R_{2020})\omega_0 - \tfrac{3}{4}\omega_1}{2\sigma_R}.$$

$\cos(3q_c x)$:

$$3\sigma R_{3030} = \sigma_R R_{3030} - R_{2020}\omega_0 - \tfrac{1}{4}\omega_1 + 64\sigma_I^{-1}\chi^2 q_c^4 R_{3030}$$

$$\left(2\sigma_R - 64\sigma_I^{-1}\right) R_{3030} = -R_{2020}\omega_0 - \tfrac{1}{4}\omega_1$$

or

$$R_{3030} = -\frac{R_{2020}\omega_0 + \tfrac{1}{4}\omega_1}{2\sigma_R - 64\sigma_I^{-1}}.$$

$\mathcal{O}\left(A_1^2 B_1\right)$:

$\cos(q_c z)$:

$$3\sigma R_{2101} - b_1 = \sigma_R R_{2101} - (2R_{2000} + R_{1111} + R_{111(-1)})\omega_0 - \tfrac{3}{2}\omega_1$$

$$2\sigma_R R_{2101} = b_1 - (2R_{2000} + R_{1111} + R_{111(-1)})\omega_0 - \tfrac{3}{2}\omega_1$$

or

$$R_{2101} = \frac{b_1 - (2R_{2000} + R_{1111} + R_{111(-1)})\omega_0 - \tfrac{3}{2}\omega_1}{2\sigma_R}.$$

$\cos[q_c(2x + z)]$:

$$3\sigma R_{2121} = \sigma_R R_{2121} - (R_{2020} + R_{1111})\omega_0 +$$

$$- \tfrac{3}{4}\omega_1 + \sigma_I^{-1}\chi^2 q_c^4 [6 + 4\cos(\psi)]^2 R_{2121}$$

$$\left(2\sigma_R - \sigma_I^{-1}[6 + 4\cos(\psi)]^2\right) R_{2121} = -(R_{2020} + R_{1111})\omega_0 - \tfrac{3}{4}\omega_1$$

or

$$R_{2121} = -\frac{(R_{2020} + R_{1111})\omega_0 + \tfrac{3}{4}\omega_1}{2\sigma_R - \sigma_I^{-1}[6 + 4\cos(\psi)]^2}.$$

$\cos[q_c(2x-z)]$:

$$3\sigma R_{212(-1)} = \sigma_R R_{212(-1)} - (R_{2020} + R_{111(-1)})\omega_0 +$$
$$-\tfrac{3}{4}\omega_1 + \sigma_I^{-1}\chi^2 q_c^4[6-4\cos(\psi)]^2 R_{212(-1)}$$
$$\left(2\sigma_R - \sigma_I^{-1}[6-4\cos(\psi)]^2\right) R_{212(-1)} = -(R_{2020} + R_{111(-1)})\omega_0 - \tfrac{3}{4}\omega_1$$

or

$$R_{212(-1)} = -\frac{(R_{2020} + R_{111(-1)})\omega_0 + \frac{3}{4}\omega_1}{2\sigma_R - \sigma_I^{-1}[6-4\cos(\psi)]^2}.$$

$\mathcal{O}\left(A_1 B_1^2\right)$:

$\cos(q_c x)$:

$$3\sigma R_{1210} - b_1 = \sigma_R R_{1210} - (2R_{0200} + R_{1111} + R_{111(-1)})\omega_0 - \tfrac{3}{2}\omega_1$$
$$2\sigma_R R_{1210} = b_1 - (2R_{0200} + R_{1111} + R_{111(-1)})\omega_0 - \tfrac{3}{2}\omega_1$$

or

$$R_{1210} = \frac{b_1 - (2R_{0200} + R_{1111} + R_{111(-1)})\omega_0 - \frac{3}{2}\omega_1}{2\sigma_R} = R_{2101}.$$

$\cos[q_c(x+2z)]$:

$$3\sigma R_{1212} = \sigma_R R_{1212} - (R_{0202} + R_{1111})\omega_0 +$$
$$- \tfrac{3}{4}\omega_1 + \sigma_I^{-1}\chi^2 q_c^4 [6 + 4\cos(\psi)]^2 R_{1212}$$
$$\left(2\sigma_R - \sigma_I^{-1}[6 + 4\cos(\psi)]^2\right) R_{1212} = -(R_{0202} + R_{1111})\omega_0 - \tfrac{3}{4}\omega_1$$

or

$$R_{1212} = -\frac{(R_{0202} + R_{1111})\omega_0 + \frac{3}{4}\omega_1}{2\sigma_R - \sigma_I^{-1}[6 + 4\cos(\psi)]^2} = R_{2121}.$$

$\cos[q_c(x-2z)]$:

$$3\sigma R_{121(-2)} = \sigma_R R_{121(-2)} - (R_{0202} + R_{111(-1)})\omega_0 +$$
$$- \tfrac{3}{4}\omega_1 + \sigma_I^{-1}\chi^2 q_c^4 [6 - 4\cos(\psi)]^2 R_{121(-2)}$$
$$\left(2\sigma_R - \sigma_I^{-1}[6 - 4\cos(\psi)]^2\right) R_{121(-2)} = -(R_{0202} + R_{111(-1)})\omega_0 - \tfrac{3}{4}\omega_1$$

or

$$R_{121(-2)} = -\frac{(R_{0202} + R_{111(-1)})\omega_0 + \frac{3}{4}\omega_1}{2\sigma_R - \sigma_I^{-1}[6 - 4\cos(\psi)]^2} = R_{212(-1)}.$$

$\mathcal{O}\left(B_1^3\right)$:

$\cos(q_c z)$:

$$3\sigma R_{0301} - a_1 = \sigma_R R_{0301} - (2R_{0200} + R_{0202})\omega_0 - \tfrac{3}{4}\omega_1$$

$$2\sigma_R R_{0301} = a_1 - (2R_{0200} + R_{0202})\omega_0 - \tfrac{3}{4}\omega_1$$

or

$$R_{0301} = \frac{a_1 - (2R_{0200} + R_{0202})\omega_0 - \tfrac{3}{4}\omega_1}{2\sigma_R} = R_{3010}.$$

$\cos(3q_c z)$:

$$3\sigma R_{0303} = \sigma_R R_{0303} - R_{0202}\omega_0 - \tfrac{1}{4}\omega_1 + 64\sigma_I^{-1}\chi^2 q_c^4 R_{0303}$$

$$\left(2\sigma_R - 64\sigma_I^{-1}\right) R_{0303} = -R_{0202}\omega_0 - \tfrac{1}{4}\omega_1$$

or

$$R_{0303} = -\frac{R_{0202}\omega_0 + \tfrac{1}{4}\omega_1}{2\sigma_R - 64\sigma_I^{-1}} = R_{3030}.$$

Landau Constants

Recall that

$$\beta_0 = \frac{(\alpha+1)^2}{\alpha-1}$$

$$\sigma_R = -1 + \frac{\beta(\alpha-1)}{(\alpha+1)^2} = -1 + \frac{\beta}{\beta_0}$$

$$\sigma_I = -1 - \frac{\beta}{\alpha+1} = -1 + \frac{\beta(\alpha+1)}{\beta_0(\alpha-1)}$$

$$\omega_0 = \frac{\beta\alpha(\alpha-3)}{(\alpha+1)^3} = \frac{\beta\alpha(\alpha-3)}{\beta_0(\alpha-1)(\alpha+1)}$$

$$\omega_1 = \frac{\beta\alpha\left[8\alpha-(\alpha+1)^2\right]}{(\alpha+1)^4} = \frac{\beta\alpha[8\alpha-(\alpha+1)^2]}{\beta_0(\alpha-1)(\alpha+1)^2}.$$

Taking the limit as $\beta \to \beta_0$, we have

$$\sigma_R[\alpha, \beta_0(\alpha)] = 0$$

$$\sigma_I[\alpha, \beta_0(\alpha)] = -1 - \frac{\alpha+1}{\alpha-1} = \frac{-2\alpha}{\alpha-1}$$

$$\omega_0[\alpha, \beta_0(\alpha)] = \frac{\alpha\,(\alpha-3)}{(\alpha-1)(\alpha+1)}$$

$$\omega_1[\alpha, \beta_0(\alpha)] = \frac{\alpha\left[8\alpha - (\alpha+1)^2\right]}{(\alpha-1)(\alpha+1)^2}$$

$$R_{2000}\Big|_{\beta=\beta_0} = \frac{\omega_0/2}{\sigma_I^{-1} - \sigma_R} = [\sigma_I\omega_0/2]\Big|_{\beta=\beta_0}$$

$$R_{2020}\Big|_{\beta=\beta_0} = \frac{\omega_0/2}{9\sigma_I^{-1} - \sigma_R} = [\sigma_I\omega_0/9]\Big|_{\beta=\beta_0}$$

$$R_{1111}\Big|_{\beta=\beta_0} = \frac{\sigma_I\omega_0}{[1+2\cos(\psi)]^2}$$

and

$$R_{111(-1)}\Big|_{\beta=\beta_0} = \frac{\sigma_I\omega_0}{[1-2\cos(\psi)]^2}.$$

Finding a_1:

$$3\sigma R_{3010} - a_1 = \sigma_R R_{3010} - (2R_{2000} + R_{2020})\omega_0 - \tfrac{3}{4}\omega_1.$$

Take $\beta \to \beta_0$:

$$\begin{aligned}
a_1 &= (2R_{2000} + R_{2020})\omega_0 + \tfrac{3}{4}\omega_1 \\
&= \frac{19}{9}\sigma_I \omega_0^2 + \frac{3}{4}\omega_1 \\
&= \frac{19}{9}\left[\frac{-\alpha}{\alpha-1}\right]\left[\frac{\alpha(\alpha-3)}{(\alpha-1)(\alpha+1)}\right]^2 + \frac{3\alpha\left[8\alpha - (\alpha+1)^2\right]}{4(\alpha-1)(\alpha+1)^2} \\
&= \frac{\alpha}{(\alpha-1)(\alpha+1)^2}\left\{-\frac{19}{9}\left[\frac{\alpha(\alpha-3)}{\alpha-1}\right]^2 + \frac{3}{4}\left[8\alpha - (\alpha+1)^2\right]\right\} \\
&= \frac{\alpha\beta_0(\alpha)}{(\alpha+1)^4}\left\{-\frac{19}{9}\left[\frac{\alpha(\alpha-3)}{\alpha-1}\right]^2 + \frac{3}{4}\left[8\alpha - (\alpha+1)^2\right]\right\}.
\end{aligned}$$

Finding b_1:

$$3\sigma R_{2101} - b_1 = \sigma_R R_{2101} - (2R_{2000} + R_{1111} + R_{111(-1)})\omega_0 - \tfrac{3}{2}\omega_1.$$

Take $\beta \to \beta_0$:

$$\begin{aligned}
b_1 &= (2R_{2000} + R_{1111} + R_{111(-1)})\omega_0 + \tfrac{3}{2}\omega_1 \\
&= \sigma_I \omega_0^2 \left[1 + \frac{1}{[1+2\cos(\psi)]^2} + \frac{1}{[1-2\cos(\psi)]^2}\right] + \frac{3\omega_1}{2} \\
&= \left[\frac{-2\alpha}{\alpha-1}\right]\left[\frac{\alpha(\alpha-3)}{(\alpha-1)(\alpha+1)}\right]^2 \left[\frac{3+16\cos^4(\psi)}{[1-4\cos^2(\psi)]^2}\right] + \frac{3\alpha\left[8\alpha-(\alpha+1)^2\right]}{2(\alpha-1)(\alpha+1)^2} \\
&= \frac{\alpha}{(\alpha-1)(\alpha+1)^2}\left\{-2\left[\frac{\alpha(\alpha-3)}{\alpha-1}\right]^2 \left[\frac{3+16\cos^4(\psi)}{[1-4\cos^2(\psi)]^2}\right] + \frac{3}{2}\left[8\alpha-(\alpha+1)^2\right]\right\} \\
&= \frac{\alpha\beta_0(\alpha)}{(\alpha+1)^4}\left\{-2\left[\frac{\alpha(\alpha-3)}{\alpha-1}\right]^2 \left[\frac{3+16\cos^4(\psi)}{[1-4\cos^2(\psi)]^2}\right] + \frac{3}{2}\left[8\alpha-(\alpha+1)^2\right]\right\}.
\end{aligned}$$

The coefficients of R

$$
\begin{aligned}
R_{2000} = R_{0200} &= -\frac{\alpha(\alpha-3)(1+\alpha+\beta)}{2(\alpha+1)(\alpha(\beta-2)-\beta-2)} \\
R_{2020} = R_{0202} &= -\frac{\alpha\beta(\alpha-3)}{2(\alpha+1)^3\left(-1+\frac{\beta(\alpha-1)}{(\alpha+1)^2}+\frac{9(\alpha+1)}{1+\alpha+\beta}\right)} \\
R_{1111} &= -\frac{\alpha\beta(\alpha-3)}{(1+\alpha)^3\left(-1+\frac{\beta(\alpha-1)}{(\alpha+1)^2}+\frac{(\alpha+1)(1+2\cos(\psi))^2}{\alpha+\beta+1}\right)} \\
R_{111(-1)} &= -\frac{\alpha\beta(\alpha-3)}{(1+\alpha)^3\left(-1+\frac{\beta(\alpha-1)}{(\alpha+1)^2}+\frac{(\alpha+1)(1-2\cos(\psi))^2}{\alpha+\beta+1}\right)} \\
R_{3010} = R_{0301} &= \frac{1}{2\left(-1+\frac{\beta(\alpha-1)}{(\alpha+1)^2}\right)}\times \\
&\quad \times\left[\frac{3\alpha\beta(1-6\alpha+\alpha^2)}{4(\alpha+1)^4}-\frac{\alpha^2\beta^2(\alpha-3)^2}{2(\alpha+1)^6}\left(\frac{2(\alpha+1)^2(1+\alpha+\beta)}{\beta(\alpha(\beta-2)+\beta+2)}+\right.\right. \\
&\quad \left.\left.-\frac{(\alpha+1)^2(1+\alpha+\beta)}{\beta(\alpha-1)(1+\alpha+\beta)+9(\alpha+1)^3-(\alpha+1)^2(1+\alpha+\beta)}\right)+a_1\right].
\end{aligned}
$$

G Stability Analysis of the Amplitude Equations

Equilibrium Points

Consider the amplitude equations

$$A' = \sigma A - A(a_1 A^2 + b_1 B^2)$$
$$B' = \sigma B - B(b_1 A^2 + a_1 B^2).$$

To find the equilibrium solutions of this system, we solve the following system of algebraic equations for A, B:

$$\sigma A - A(a_1 A^2 + b_1 B^2) = 0$$
$$\sigma B - B(b_1 A^2 + a_1 B^2) = 0.$$

(i) Trivial solution: $A = B = 0$.

(ii) Let $B = 0$ and $A \neq 0$. Then

$$\sigma - a_1 A^2 = 0,$$

that is,

$$A^2 = \frac{\sigma}{a_1}.$$

(iii) Similarly, another solution is

$$A = 0, \quad B^2 = \frac{\sigma}{a_1}.$$

(iv) Assume $A \neq 0$ and $B \neq 0$. Then our system takes the form

$$\sigma - (a_1 A^2 + b_1 B^2) = 0$$
$$\sigma - (b_1 A^2 + a_1 B^2) = 0,$$

which implies

$$a_1 A^2 + b_1 B^2 = b_1 A^2 + a_1 B^2,$$

and so $A^2 = B^2$, if we assume also that $a_1 \neq b_1$. Then,

$$\sigma - (a_1 + b_1) A^2 = 0,$$

and thus

$$A^2 = \frac{\sigma}{a_1 + b_1}.$$

Stability Analysis

Assuming that $a_1 + b_1 > 0$, we seek a solution of the form

$$A_1(t) = A_0 + \varepsilon c_1 \mathrm{e}^{pt} + \mathcal{O}\left(\varepsilon^2\right)$$
$$B_1(t) = B_0 + \varepsilon c_2 \mathrm{e}^{pt} + \mathcal{O}\left(\varepsilon^2\right).$$

We have

$$A_1'(t) = \varepsilon p c_1 \mathrm{e}^{pt} + \mathcal{O}\left(\varepsilon^2\right)$$
$$B_1'(t) = \varepsilon p c_2 \mathrm{e}^{pt} + \mathcal{O}\left(\varepsilon^2\right).$$

Substituting in our equations:

$$\begin{aligned}
\varepsilon p c_1 \mathrm{e}^{pt} &= \sigma\left[A_0 + \varepsilon c_1 \mathrm{e}^{pt} + \mathcal{O}\left(\varepsilon^2\right)\right] - \left[A_0 + \varepsilon c_1 \mathrm{e}^{pt} + \mathcal{O}\left(\varepsilon^2\right)\right] \cdot \\
&\qquad \cdot \left[a_1\left(A_0 + \varepsilon c_1 \mathrm{e}^{pt} + \mathcal{O}\left(\varepsilon^2\right)\right)^2 + b_1\left(B_0 + \varepsilon c_2 \mathrm{e}^{pt} + \mathcal{O}\left(\varepsilon^2\right)\right)^2\right] + \mathcal{O}\left(\varepsilon^2\right) \\
&= \sigma\left(A_0 + \varepsilon c_1 \mathrm{e}^{pt}\right) - \left(A_0 + \varepsilon c_1 \mathrm{e}^{pt}\right) \cdot \\
&\qquad \cdot \left[a_1\left(A_0^2 + 2\varepsilon A_0 c_1 \mathrm{e}^{pt}\right) + b_1\left(B_0^2 + 2\varepsilon B_0 c_2 \mathrm{e}^{pt}\right)\right] + \mathcal{O}\left(\varepsilon^2\right) \\
&= \sigma A_0 - A_0(a_1 A_0^2 + b_1 B_0^2) + \\
&\qquad + \varepsilon\left(\sigma c_1 - 2a_1 A_0^2 c_1 - a_1 A_0^2 c_1 - 2b_1 A_0 B_0 c_2 - b_1 B_0^2 c_1\right)\mathrm{e}^{pt} + \mathcal{O}\left(\varepsilon^2\right) \\
&= \varepsilon\left[\left(\sigma - 3a_1 A_0^2 - b_1 B_0^2\right)c_1 - 2b_1 A_0 B_0 c_2\right]\mathrm{e}^{pt} + \mathcal{O}\left(\varepsilon^2\right),
\end{aligned}$$

and

$$\begin{aligned}
\varepsilon p c_2 \mathrm{e}^{pt} &= \sigma\left[B_0 + \varepsilon c_2 \mathrm{e}^{pt} + \mathcal{O}\left(\varepsilon^2\right)\right] - \left[B_0 + \varepsilon c_2 \mathrm{e}^{pt} + \mathcal{O}\left(\varepsilon^2\right)\right] \cdot \\
&\quad \cdot \left[a_1\left(B_0 + \varepsilon c_2 \mathrm{e}^{pt} + \mathcal{O}\left(\varepsilon^2\right)\right)^2 + b_1\left(A_0 + \varepsilon c_1 \mathrm{e}^{pt} + \mathcal{O}\left(\varepsilon^2\right)\right)^2\right] + \mathcal{O}\left(\varepsilon^2\right) \\
&= \sigma\left(B_0 + \varepsilon c_2 \mathrm{e}^{pt}\right) - \left(B_0 + \varepsilon c_2 \mathrm{e}^{pt}\right) \cdot \\
&\quad \cdot \left[a_1\left(B_0^2 + 2\varepsilon B_0 c_2 \mathrm{e}^{pt}\right) + b_1\left(A_0^2 + 2\varepsilon A_0 c_1 \mathrm{e}^{pt}\right)\right] + \mathcal{O}\left(\varepsilon^2\right) \\
&= \sigma B_0 - B_0(a_1 B_0^2 + b_1 A_0^2) + \\
&\quad + \varepsilon\left(\sigma c_2 - 2a_1 B_0^2 c_2 - a_1 B_0^2 c_2 - 2b_1 A_0 B_0 c_1 - b_1 A_0^2 c_2\right)\mathrm{e}^{pt} + \mathcal{O}\left(\varepsilon^2\right) \\
&= \varepsilon\left[\left(\sigma - 3a_1 B_0^2 - b_1 A_0^2\right)c_2 - 2b_1 A_0 B_0 c_1\right]\mathrm{e}^{pt} + \mathcal{O}\left(\varepsilon^2\right).
\end{aligned}$$

After neglecting terms of $\mathcal{O}\left(\varepsilon^2\right)$ and cancelling the common factor e^{pt}, we obtain the following system of linear equations in $\{c_1, c_2\}$:

$$\begin{aligned}
\left[(p - \sigma) + 3a_1 A_0^2 + b_1 B_0^2\right] c_1 + 2b_1 A_0 B_0 c_2 &= 0 \\
\left[(p - \sigma) + 3a_1 B_0^2 + b_1 A_0^2\right] c_2 + 2b_1 A_0 B_0 c_1 &= 0,
\end{aligned}$$

which has nontrivial solutions when

$$\det\begin{bmatrix} p - \alpha & \gamma \\ \gamma & p - \beta \end{bmatrix} = 0,$$

with

$$\alpha = \sigma - 3a_1 A_0^2 - b_1 B_0^2$$
$$\beta = \sigma - 3a_1 B_0^2 - b_1 A_0^2$$

and

$$\gamma = 2b_1 A_0 B_0.$$

(a) For $A_0 = B_0 = 0$, we have $\alpha = \beta = \sigma$ and $\gamma = 0$, so the solutions are

$$p_{1,2} = \sigma,$$

and thus the solid pattern I is stable for $\sigma < 0$.

(b) For $A_0^2 = \sigma/a_1$, $B_0 = 0$, we have $\alpha = -2\sigma$, $\beta = (1 - b_1/a_1)\sigma$ and $\gamma = 0$, so the roots are

$$p_1 = \alpha = -2\sigma,$$
$$p_2 = \beta = \left(1 - \frac{b_1}{a_1}\right)\sigma,$$

which implies that the stripe-type pattern II is stable when $\sigma > 0$ and $b_1 > a_1$.

(c) Finally, for $A_0^2 = B_0^2 = \sigma/(a_1 + b_1)$, we have $\alpha = \beta$ and $\gamma \neq 0$, so the solutions are

$$\begin{aligned} p_1 &= \alpha - \gamma \\ &= \sigma - (3a_1 + b_1)A_0^2 - 2b_1A_0^2 \\ &= \sigma - 3(a_1 + b_1)A_0^2 \\ &= \sigma - \frac{3(a_1 + b_1)\sigma}{a_1 + b_1} \\ &= -2\sigma \end{aligned}$$

and

$$\begin{aligned} p_2 &= \alpha + \gamma \\ &= \sigma - (3a_1 + b_1)A_0^2 + 2b_1A_0^2 \\ &= \sigma - (3a_1 - b_1)A_0^2 \\ &= \sigma - \frac{(3a_1 - b_1)\sigma}{a_1 + b_1} \\ &= \frac{[(a_1 + b_1) - (3a_1 - b_1)]\sigma}{a_1 + b_1} \\ &= \frac{2(b_1 - a_1)\sigma}{a_1 + b_1}, \end{aligned}$$

which implies that the rhombic-type pattern V is stable when $\sigma > 0$ and $b_1 < a_1$.

REFERENCES

[1] T. Ackemann, Yu A. Logvin, A. Heur, and W. Lange. Transition between positive and negative hexagons in optical pattern formation. *Physical Review Letters*, 75:3450–3453, 1995.

[2] Dean E. Edmeade. *Nonlinear Stability Analysis of Hexagonal Optical Pattern Formation in an Atomic Sodium Vapor Ring Cavity*. PhD thesis, Washington State University, 2004.

[3] W. J. Firth and A. J. Scroggie. Spontaneous pattern formation in an absorptive system. *Europhysics Letters*, 26:521–526, 1994.

[4] J. B. Geddes, R. A. Indik, J. V. Moloney, and W. J. Firth. Hexagons and squares in a passive nonlinear optical system. *Physical Review A*, 50:3471–3485, 1994.

[5] E. L. Koschmieder, editor. *Bénard Cells and Taylor Vortices*. Cambridge University Press, Cambridge, 1993.

[6] L. A. Lugiato and R. LeFever. Spatial dissipative structures in passive optical systems. *Physical Review Letters*, 58:2209–2211, 1987.

[7] L. A. Lugiato and C. Oldano. Stationary spatial patterns in passive optical systems: Two-level atoms. *Physical Review A*, 37:3896–3908, 1988.

[8] Phillip K. Maini and Hans G. Othmer, editors. *Mathematical Models for Biological Pattern Formation*, volume 121 of *The IMA Volumes in Mathematics and its Applications: Frontiers in Applications of Mathematics*. Springer, 2001.

[9] A. V. Mammaev and M. Saffman. Hexagonal optical patterns in anisotropic nonlinear media. *Europhysics Letters*, 34:669–674, 1996.

[10] P. Mandel, M. Georgiou, and T. Erneux. Transverse effects in coherently driven nonlinear cavities. *Physical Review A*, 47:4277–4286, 1993.

[11] Lee A. Segel. The nonlinear interaction of a finite number of disturbances in a layer of fluid heated from below. *Journal of Fluid Mechanics*, 21:359–384, 1965.

[12] James Victor Uspensky. *Theory of Equations*. McGraw-Hill, New York, New York, 1948.

[13] David J. Wollkind, Valipuram S. Manoranjan, and L. Zhang. Weakly nonlinear stability analyses of prototype reaction-diffusion model equations. *SIAM Review*, 36:176–214, 1994.

[14] David J. Wollkind, R. Sriranganathan, and D. B. Oulton. Interfacial patterns during plane front alloy solidification. *Physica D*, 12:215–240, 1984.

[15] David J. Wollkind and Laura E. Stephenson. Chemical Turing pattern formation analyses: Comparison of theory with experiment. *SIAM Journal on Applied Mathematics*, 61:387–431, 2000.